Acta Universitatis
Lappeenrantaensis
831

Simo Kalliola

MODIFIED CHITOSAN NANOPARTICLES AT LIQUID-LIQUID INTERFACE FOR APPLICATIONS IN OIL-SPILL TREATMENT

Simo Kalliola

MODIFIED CHITOSAN NANOPARTICLES AT LIQUID-LIQUID INTERFACE FOR APPLICATIONS IN OIL-SPILL TREATMENT

Thesis for the degree of Doctor of Science (Technology) to be presented with due permission for public examination and criticism in the Mikaeli Concert and Congress Hall, Mikkeli, Finland on the 10th of December, 2018, at noon.

Acta Universitatis
Lappeenrantaensis 831

Supervisors Professor Mika Sillanpää
LUT School of Engineering Science
Lappeenranta University of Technology
Finland

Associate professor Eveliina Repo
LUT School of Engineering Science
Lappeenranta University of Technology
Finland

Reviewers Professor Michael K.C. Tam
Department of Chemical Engineering
University of Waterloo
Canada

Professor Orlin D. Velev
Department of Chemical and Biomolecular Engineering
North Carolina State University
USA

Opponent Dr. Roman Netzer
SINTEF Ocean
Norway

ISBN 978-952-335-308-4
ISBN 978-952-335-309-1 (PDF)
ISSN-L 1456-4491
ISSN 1456-4491

Lappeenrannan teknillinen yliopisto
Yliopistopaino 2018

Abstract

Simo Kalliola

Modified chitosan nanoparticles at liquid-liquid interface for applications in oil-spill treatment

Lappeenranta 2018
45 pages
Acta Universitatis Lappeenrantaensis 831
Diss. Lappeenranta University of Technology
ISBN 978-952-335-308-4, ISBN 978-952-335-309-1 (PDF), ISSN-L 1456-4491, ISSN 1456-4491

Oil-spills continue to be a serious threat to the environment and the climate change is expected to increase oil related industry and transportation in Arctic regions due to the melting of the ice cover. Nanoparticles prepared from renewable, biodegradable and non-toxic biopolymers could provide feasible alternative to traditionally used molecular dispersants which are toxic. Chitosan is a renewable, biodegradable and non-toxic polysaccharide derived from the shells of crustacean, for example. A biodegradable and non-toxic chitosan derivative carboxymethyl chitosan was synthesized and used to prepare nanoparticles with and without cross-linking using $CaCl_2$. The $CaCl_2$ cross-linked nanoparticles were fairly stable in increased NaCl concentration and could be made stable in varying pH (7-9) by adjusting the pH during the preparation of the nanoparticles. The nanoparticles could adsorb into the oil-water interface and stabilize emulsions. The non-cross-linked nanoparticles were formed by adjusting pH close to the pI value of carboxymethyl chitosan. The nanoparticles could form gel-like emulsions with oil, and the emulsification was reversible by pH adjustment due to the dissolution of the particles. Additional hydrophobic modification increased the emulsification ability of the nanoparticles. Also, vanillin grafted chitosan particles were synthesized and studied for oil emulsification. The particles aggregated upon mixing with oil and encapsulated small droplets with in the aggregates effectively separating the oil from the aqueous phase.

Keywords: Chitosan, carboxymethyl chitosan, nanoparticle, liquid-liquid interface, emulsions, oil

Acknowledgements

This research for a doctoral thesis was carried out in the Laboratory of Green Chemistry, Lappeenranta University of Technology from 2014 to 2018. The work was financially supported by Academy of Finland, and was part of a joint project between University of Oulu and Lappeenranta University of Technology. I'm very grateful to my supervisor professor Mika Sillanpää for this opportunity to do my PhD and for his guidance during this project. I'm also grateful to Dr. Eveliina Repo for her supervision and guidance during the project.

I'm grateful to professor Michael K.C. Tam and professor Orlin D. Velev for reviewing my thesis, and to Dr. Roman Netzer for acting as an opponent.

I'm grateful to professor Vijay T. John, Dr. Jaspreet Arora, Dr. Jibao He, and everyone else in Tulane University for very educational and pleasant visit in New Orleans during the summer 2015. Thank you also to our collaborators in University of Oulu, Dr. Henrikki Liimatainen, Jonna Ojala, Dr. Juha Heiskanen, and Dr. Juho Sirviö, for interesting and helpful discussions. Also, I'd like to thank my friends and colleagues Dr. Feiping Zhao, Dr. Jean-Marie Fontmorin, Dr. Evgenia Iakovleva, Dr. Sara-Maaria Alatalo, Dr. Yunfan Zhang, Bhairavi Doshi, and everyone else in the Laboratory of Green Chemistry. Thank you to my family and especially to my fiancée Dr. Marina Shestakova for support during this work and otherwise in life.

Simo Kalliola
January 2018
Finland

Contents

Abstract ... 3
Acknowledgements ... 5
Contents ... 7
List of publications ... 9
List of symbols and abbreviations ... 10
1 Introduction ... 11
1.1 Oil-spills ... 11
1.2 Oil-spill treatment ... 11
1.3 Particle adsorption to liquid-liquid interface ... 13
1.3.1 Spherical particles ... 13
1.3.2 Non-spherical particles ... 15
1.4 Charged particles at liquid-liquid interface ... 16
1.5 Soft particles at liquid-liquid interface ... 16
1.6 Janus particles at liquid-liquid interface ... 17
1.6.1 Spherical Janus particles ... 17
1.6.2 Non-spherical Janus particles ... 18
1.7 Emulsions stabilized by particles ... 19
1.7.1 Size, shape, and concentration ... 19
1.7.2 Wettability ... 19
1.7.3 Particle-particle interactions ... 20
1.7.4 Oil and aqueous phase properties ... 21
1.8 Chitin, chitosan, and other selected polysaccharides ... 21
1.8.1 Polysaccharides ... 21
1.8.2 Chitin and Chitosan ... 22
1.8.3 Cellulose ... 22
1.8.4 Starch ... 23
1.8.5 Alginate ... 23
1.9 Synthesis of polysaccharide nanoparticles by selected methods ... 23
1.9.1 Self-assembly methods ... 23
1.9.2 Ionic gelation of polyelectrolyte ... 24
1.9.3 Complex coacervation method ... 24
1.9.4 Desolvation/precipitation method ... 24
1.9.5 Emulsification method ... 24
1.9.6 Isolation of nanocrystals ... 25
1.10 Chitosan nanoparticles ... 25

1.10.1 Synthesis of chitosan nanoparticles 25
1.10.2 Chitosan nanoparticles at liquid-liquid interface 26
1.11 Carboxymethyl chitosan 27
1.11.1 Properties of carboxymethyl chitosan 27
1.11.2 Synthesis by reductive alkylation using aldehydes 27
1.11.3 Synthesis by direct alkylation using monochloroacetic acid 27
1.12 Carboxymethyl chitosan nanoparticles 27
2 Research objectives 29
3 Materials and methods 29
3.1 Synthesis of chitosan derivatives and their nanoparticles 29
3.1.1 Carboxymethyl chitosan 29
3.1.2 Hydrophobically modified carboxymethyl chitosan 30
3.1.3 Vanillin-chitosan 30
3.2 Characterizations 30
4 Results and discussion 31
4.1 Carboxymethyl chitosan nanoparticles and their properties 31
4.2 Carboxymethyl chitosan nanoparticles in contact with liquid-liquid interface 32
5 Conclusion and further research 37
6 References 39

List of publications

I. Kalliola S., Repo E., Sillanpää M., Arora J.S., He J., John V.T., The stability of green nanoparticles in increased pH and salinity for applications in oil spill-treatment, *Colloids and Surfaces A: Physicochemical and Engineering Aspects* 493 (2015) 99-107.

II. Kalliola S., Repo E., Srivastava V., Heiskanen J.P., Sirviö J.A., Liimatainen H., Sillanpää M., The pH sensitive properties of carboxymethyl chitosan nanoparticles cross-linked with calcium ions, *Colloids and Surfaces B: Biointerfaces* 153 (2016) 229-236.

III. Kalliola S., Repo E., Srivastava V., Zhao F., Heiskanen J.P., Sirviö J.A., Liimatainen H., Sillanpää M., Carboxymethyl chitosan and its hydrophobically modified derivative as pH-switchable emulsifiers, *Langmuir* 34(8) (2018) 2800–2806.

IV. Kalliola S., Repo E., Zhao F., Srivastava V., Sillanpää M., Vanillin substituted chitosan particles applied to oil/water separation, Submitted to *Reactive and Functional Polymers*

Author's contribution

Simo Kalliola is the principal author and investigator in papers I-IV.

List of symbols and abbreviations

G_{ads} = adsorption free energy
γ_{12} = interfacial tension between liquid phases 1 and 2
γ_{1S} = interfacial tension between liquid phases 1 and solid phase
γ_{2S} = interfacial tension between liquid phases 2 and solid phase
A_{12} = area of the liquid-liquid interface displaced by the adsorb particle
A_{1S} = area of the particle in contact with liquid phase 1
A_{2S} = area of the particle in contact with liquid phase 2
θ_1 = contact angle of the particle towards liquid phase 1
θ_2 = contact angle of the particle towards liquid phase 2
k = Boltzmann constant ($1.38064852 \times 10^{-23}$ m^2 kg s^{-2} K^{-1})
T = temperature
O/W = oil-in-water emulsion
W/O = water-in-oil emulsion
W/W = water-in-water emulsion
W/W/O = water-in-water-in-oil emulsion
W/O/W = water-in-oil-in-water emulsion
TPP = sodium tripolyphosphate
M = β(1,4)-linked D-mannuronic acid
G = α(1,4)-linked L-guluronic acid
TEMPO = 2,2,6,6-tetramethyl-piperidinyl-1-oxyl
pI = isoelectric point
CMC = *N*,*O*-carboxymethyl chitosan
CMC-Ca = *N*,*O*-carboxymethyl chitosan nanoparticle cross-linked with Ca^{2+} ions

1 Introduction

1.1 Oil-spills

Oil-spill refers to environmental pollution due to liquid petroleum hydrocarbons released into the environment. The term may include both marine and land oil-spills but this work discusses only marine oil spills, and therefore, here the term oil-spill refers to only marine oil-spills, unless otherwise noted.

Crude oil is a complex mixture of hydrocarbons of varying molecular weights and structures, such as alkanes, cycloalkanes and aromatic compounds [1, 2, 3]. The crude oil also contains other organic compounds with nitrogen, oxygen, and sulfur elements, and small amounts of metals [3, 4, 5]. Due to the complex composition of the crude oil and the complexity and diversity of the marine ecosystems, all the effects of oil-spills to environment, humans, and animals are not known [6, 4]. The oil is not limited to just crude oil, it can be also other oily substances or refined petroleum products, such as diesel and gasoline [3].

In case of an oil-spill, the oil at the surface of the water can spread to a very large area as a thin oil slick. As the oil spreads the surface area of the oil increases and the evaporation of the volatile fraction increases. The volatile fraction of the oil is usually the least dense, and the evaporation increases the total density of the oil, due to the evaporation of the lower density fraction. Also, some fraction of the oil is water-soluble and dissolves into the water body. As the overall density of the oil increases, the heavier and denser fractions of the oil sink to the bottom of the sea or lake where it can damage the eco-system not to mention that the removal of such oil is extremely difficult. [1]

Oil-spills can have immediate environmental and economic impact [7]. In 2010, the Deepwater Horizon oil-spill in the Gulf of Mexico released several hundred tons of crude oil into the environment. [6, 3] The accident is considered as one of the largest oil-spills in history [8, 3] resulting in significant damage to the biodiversity and environment. The oil-spill caused also air pollution in the coastal area due to the evaporated components of the crude oil [6]. But in general, the size of the oil-spill does not correlate well with the environmental impact. A small oil-spill can have a large impact on the biodiversity if the ecosystem is sensitive in the area of occurrence. For example, arctic region has sensitive ecosystems, and harsh weather conditions and remote locations can limit the available oil-spill treatment methods [9, 10]. The shipping of oil products is likely to increase in the arctic region, due to the climate change and the melting of the ice cover. Increased oil related industrial activity in the area is going to increase the risk of an oil-spill. Therefore, there is a need for fast and effective oil-spill treatment methods.

1.2 Oil-spill treatment

In case of an oil-spill, a suitable treatment method needs to be chosen. Different methods have their strengths and weaknesses [3], and the suitability depends on the weather conditions, location, and size of the oil-spill, for example. Rapid oil-spill treatment methods are needed to prevent the oil from spreading and damaging the environment. Different kind of treatment methods have been reported in literature and different authors use slightly different categorizations, but the oil-spill treatment methods can be categorized generally as biological, physical, in-situ burning, and chemical. [3, 11, 12] The main differences are in the separation

of physical and chemical methods. Strictly speaking, the only method usually involving chemical reactions is in-situ burning of oil i.e. oil is transformed into mainly CO_2. All other methods are physical in sense that they mechanically remove the oil from the environment using mechanical devices or they change the physical state of the oil through, for example, dissolution of chemical agents or adsorption of oil. Here, the chemical methods include all the methods involving addition of materials or chemical agents into the environment and physical methods include all the mechanical methods that aim to remove the oil from the environment.

The first option is to let the native micro-organisms biodegrade the oil. This option may be suitable only for small scale oil-spills since the biodegradation is slow and can take years [3, 13, 14] especially in cold climate [15, 16] but biodegradation does occur even in the Arctic [9]. The biodegradation can be enhanced by addition of biological agents or nutrients into the oil-spill [3].

Physical methods include variety of booms and skimmers that are used to mechanically contain and remove the oil [3, 4]. Recently, there has been variety of different kind of specially wettable materials reported in literature that can either let the oil pass through it and keep the water out or let the water pass through and keep the oil out [17, 18, 19]. These kind of materials could be used for skimming of the oil from the water surface [20]. Mechanical methods are slow and require suitable weather conditions to be effective. Also, after the oil is gathered into a thick slick using mechanical devices it can be burned on site. [3, 4] The burning of oil can reduce the amount of oil in the marine environment but the oil slick needs to be sufficiently thick for the burning to be effective. Also, the burning causes air pollution, such as sooth and CO_2. [3, 21]

Chemical methods include all the methods that involve addition of chemical agents into the oil-spill. The chemical agents can have different effects on the oil, such as immobilization or dispersion [3]. The oil can be immobilized with suitable materials, such as sorbents or gelators. Both sorbents and gelators have been classified as solidifiers, although there is no widely accepted definition for a solidifier [11]. The mechanisms of sorption and gelation are also very different. In sorption, the oil is attached to the solid sorbent through sorption, and the sorbent can be removed from the water [22, 3, 23]. Variety of inorganic [24], synthetic organic [25], and natural materials [26] have been studied for oil sorption in oil-spill treatment. Recently, increasing attention has been given to aerogels as sorbents for oil-spill treatment [27, 28, 29, 23]. Aerogels are gels where the liquid portion of the gel has been replaced by air resulting in highly porous solid material with high specific surface area and low density. These attributes are ideal to be utilized as oil sorbents due to their high potential sorption capacity and good buoyancy properties [27]. Although, the high cost of the preparation limits their practical use. Gelators turn the oil into a semi-solid allowing more easy removal from water [30, 11]. Gelators can be divided into polymeric gelators (PG) and low-molecular-weight gelators (LMWG) [11, 31]. Gelation using PGs is achieved through the formation of covalent or non-covalent cross-linking by long-chain polymers [32]. On the other hand, LMWGs self-assemble into cross-linked fibers to form a gel network [33]. In the past, gelators (solidifiers) have not been used extensively due to the large amount of gelator needed to gelate the oil [3, 34] and dispersants are relatively more effective [3]. Recently, increasing attention have been focused on sugar based phase-selective LMWGs as green chemicals that form gels only with oil and are insoluble in water [35, 36, 37].

The oil can be dispersed with surfactants [38, 39, 3], polymers [40, 41], or particles [42, 43, 44]. These species can attach to the oil-water-interface and stabilize oil-in-water emulsions.

The formation of stable oil droplets breaks down the oil slick and the oil droplets are dispersed and diluted into the water body to enhance the biodegradation. Surfactants are in equilibrium between adsorbed and desorbed species [45, 46]. Therefore, the surfactants may desorb from the oil-water interface as the droplets are diluted into the water body resulting in the destabilization of the droplets and subsequent coalescence. This can be hindered by addition of water soluble polymers with hydrophobic side-chains [40]. These kind of polymers can attach to the oil-water interface and stay adsorbed since at least some of the side-chains are always adsorbed into the interface. Particles can also adsorb at the oil-water interface and stabilize oil-in-water emulsions [42], and similarly disperse the oil into the water body. The adsorption of particles is usually stronger than surfactant molecules and can be regarded as "irreversible" resulting in more stable emulsions.

1.3 Particle adsorption to liquid-liquid interface

1.3.1 Spherical particles

The solid particle needs to be partially wetted by water and oil for it to be possible to adsorb at the oil-water interface. A very hydrophilic particle would not be able to adsorb at the interface since it would be completely wetted and dispersed in aqueous phase. Similarly, a very hydrophobic particle would not be able to adsorb since it would be completely wet by oil. The adsorption is determined by the interfacial tension between the immiscible liquids (γ_{12}), and the interfacial tensions between the liquid phases and the solid phase (γ_{1S} and γ_{2S}). The contact angles (θ_1, θ_2) between the liquid phases and the solid surface depend on the interfacial tensions between the three phases according to Young's equation (1). [47]

$$\cos\theta_1 = \frac{\gamma_{1S}-\gamma_{2S}}{\gamma_{12}} = \frac{-\gamma_{1S}+\gamma_{2S}}{\gamma_{12}}\cos\theta_2\,,\theta_2 = \pi - \theta_1 \qquad (1)$$

As a particle adsorbs at the liquid-liquid interface, it changes the free energy of the system since the balance of interfacial energies is changed (Figure 1.). The particle reduces the interfacial area between the two immiscible liquids, and the solid particle surface comes in contact with both of the liquid phases. The adsorption free energy (G_{ads}) is thus the sum of the interfacial energies between the solid phase and two liquid phases, and the interfacial energy associated with the displaced area between the two liquid phases. [48] Therefore, G_{ads} for a particle adsorbed on the interface depends on the area of the liquid-liquid interface displaced by the adsorb particle (A_{12}), and the contact area of the solid phase with the two liquid phases (A_{1S} and A_{2S}) in addition to the interfacial tensions between the three phases according to Equation (2).

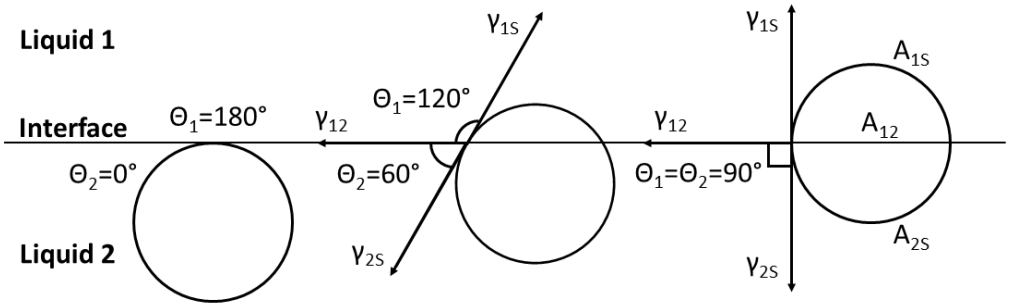

Figure 1. Particle at liquid-liquid interface. Contact angles of the particle (θ_1 and θ_2), liquid-liquid interfacial tension (γ_{12}), liquid-solid interfacial tensions (γ_{1S} and γ_{2S}), liquid-liquid surface area (A_{12}), and the liquid-solid surface areas (A_{1S} and A_{2S}) are presented.

$$G_{ads} = \gamma_{12}A_{12} + \gamma_{1S}A_{1S} + \gamma_{2S}A_{2S} \quad (2)$$

For a spherical, perfectly smooth, and rigid particle with homogeneous wettability the equation (2) takes the form of equation (3). The energy required to remove the particle from the interface depends on the interfacial tension between the liquids (γ_{12}), the size of the particle (radius r), and the contact angle ($\theta_{12} = \theta_1$ or θ_2). [49]

$$G_{ads} = \pi r^2 \gamma_{12}(1 - |\cos(\theta_{12})|)^2 \quad (3)$$

The equation states that adsorption energy is at maximum when the contact angle is 90° i.e. the particle is equally wetted by oil and aqueous phases since at this position in the interface the particle displaces the maximum amount of the interfacial area between the two liquids. Also, for the same reason, the adsorption energy increases as the size of the particle increases. Similarly, at contact angle close to 0° or 180°, the particle barely touches the interface and the adsorption energy is negligible. [48] The value of G_{ads} is plotted using equation (3) for a particle with diameter 100, 50, and 10 nm in Figure 2.

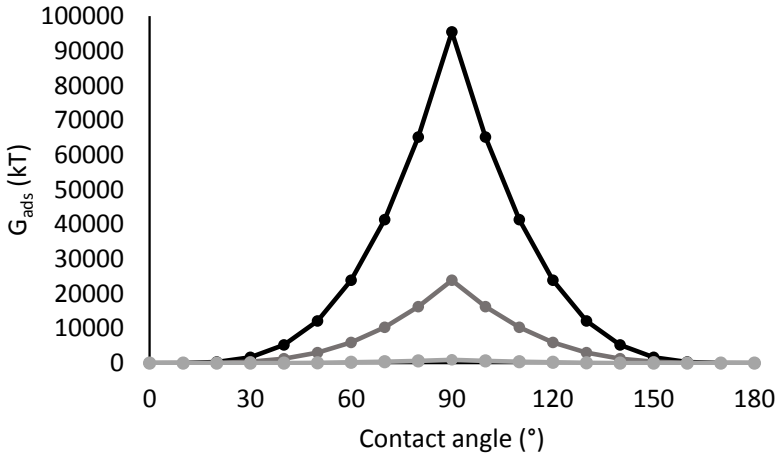

Figure 2. Free energy of adsorption of a spherical particle at the liquid-liquid interface (γ_{12} = 50 mN/m) at 298 K. Diameter of the particle from top to bottom: 100, 50, 10 nm.

Although, the adsorption energy is higher with large particles, it is already very high with very small particles. For example, even for a spherical particle with diameter of 100 nm, at oil-water interface (γ_{12} = 50 mN/m) with contact angle of 90°, the energy is approximately 10^5 kT at 298 K i.e. several orders of magnitude larger than thermal energy. The adsorption energy decreases rapidly as the contact angle is decreased, but even at 30°, the energy is still 10-10^3 kT with particle radius of 10-100 nm, respectively. Therefore, the particles are "irreversibly" adsorbed at the oil-water interface since the amount of energy required to remove the particle from the surface is many orders of magnitude larger than the thermal energy and random fluctuations are not sufficient to remove the particle from the interface in most cases. In contrast, traditional surfactants are reversibly adsorbed at the liquid-liquid interface and in rapid dynamic equilibrium between adsorbed and desorbed species [45, 46]. The particles do not lower the interfacial tension like traditional surfactant molecules [47, 45, 49]. There have been some controversy about the interfacial tension reduction in the literature, but the reduction in interfacial tension can be explained by soluble residues i.e. impure samples [49].

1.3.2 Non-spherical particles

Generally, the non-spherical i.e. anisotropic particles adapt the orientation at the liquid-liquid interface that maximizes the displaced area at the interface [50]. For example, long cylinder shaped particles prefer a horizontal orientation at the interface. This general rule applies also to other shapes, such as ellipsoids, dumbbells (two particles fused together), and complex-shaped particles. [48] For particles with geometries other than sphere, the equation of adsorption energy can be derived from equation (2). For example, energy to remove a cylindrical particle is presented in Equation (4).

$$G_{ads} = 2rL\gamma_{12}\left[\sin\theta - \theta\cos\theta\left(1 + \frac{r}{L}\right) + \frac{r\cos^2\theta\sin\theta}{L}\right] \quad (4)$$

Where r is the radius of the cylinder, L is the length of the cylinder, θ is the contact angle of the cylinder, and γ_{12} is the interfacial tension at liquid-liquid interface [42].

Anisotropic particles usually distort the interface around the particle from its planar state due to the particle shape, except perfectly smooth spherical particles, capsule shaped particles, or perfectly flat particles. The distortion of the interface can also be induced by surface roughness or chemical heterogeneity. Capillary interactions are induced by the overlapping of the distortions created by two or more anisotropic particles to reduce the total energy of the system (Figure 3.). Identical deformations of the interface attract and opposite deformations repel. This is analogous to positive and negative electric charges except in this case similar "charges" attract and opposite "charges" repel. The capillary interactions have relatively long range and their strength is comparable to or greater than non-covalent interactions such as van der Waals and dipole-dipole interactions. The strength of the capillary interactions depends on the size of the particle. The capillary interactions are comparable to kT when the particle is approximately 1-10 nm in diameter, but as the size of the particle is increased to 1000 nm the capillary interactions are in the order of 10^6 kT. The curvature of the interface also affects the capillary interactions, such as on the droplet surface. On a curved interface, perfectly smooth and spherical particles distort the interface due to the curvature of the interface and exhibit capillary interactions. For anisotropic particles, the curvature affects the assembly of the particle in the interface. [48]

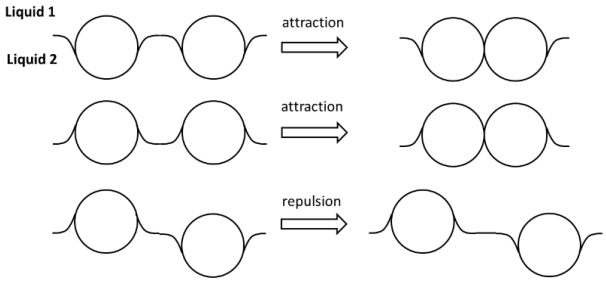

Figure 3. Capillary distortions generating attraction and repulsion between particles.

1.4 Charged particles at liquid-liquid interface

Often, colloidal particles are dispersed in aqueous phase due to surface charge induced by dissociating functional, such as carboxyl groups, at the particle surface. At the fluid-fluid interface, the surface groups may be neutralized depending on the dielectric constant of the non-aqueous phase (Figure 4.). If the non-aqueous phase is non-polar fluid, such as air with dielectric constant ≈ 1, the functional groups in contact with air are neutralized. If the non-aqueous phase is an oil, it is not clear whether the charges are neutralized or not, if the dielectric constant of the oil is low ≈ 2. But for oils with high dielectric constant ≈ 5 the surface charges can be stable at the particle surface in contact with the oil. Interactions between micrometer sized particles at the interface are direct, such as electric, magnetic, or elastic, which are present also in the bulk phase but the interactions behave differently at the interface. Indirect capillary interactions can be induced by the direct interactions in addition to the anisotropic shape of the particle. The direct interactions generate forces to the particles that deform the liquid-liquid interface inducing the capillary interactions. Charged colloidal particles induce deformation on the interface causing attractive electrocapillary interactions. Nanometer sized particles are expected to behave mostly similar to micrometersized particles but very small particle may be affected by the thermal fluctuations of the interface. [51]

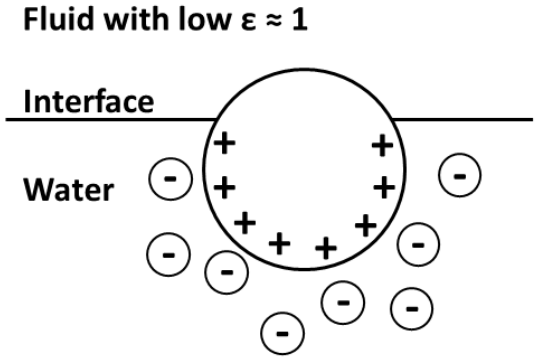

Figure 4. Charged particle in a fluid-water interface with partially neutralized surface groups.

1.5 Soft particles at liquid-liquid interface

The adsorption of particles, both perfectly soft (liquid droplets) and perfectly rigid, is determined by the interfacial tensions between the three phases, γ_{12}, γ_{1S}, γ_{2S}. Soft particles can spread at the liquid-liquid interface to displace more of the interfacial area than a similar volume rigid spherical particle (Figure 5.). The spreading of the particle is characterized by

contact radius (a) with the interface, and its ratio to the original radius (r) of the particle. The ratio a/r depends only on the ratios of the interfacial tensions γ_{1S}/γ_{12} and γ_{2S}/γ_{12}. Both rigid and soft particles adsorb similarly to the interface when the value of γ_{1S}/γ_{12} or γ_{2S}/γ_{12} are high, since large interfacial tension between the particle and either of the liquid phases (compared to the liquid-liquid interfacial tension) keeps the soft particles approximately spherical. The difference between soft and rigid particles arises when γ_{1S}/γ_{12} and γ_{2S}/γ_{12} are small i.e. the liquid-liquid interfacial tension is high compared to the solid-liquid interfacial tensions. In this case, the soft particle can spread due to liquid-liquid interfacial tension and the deformed particle displaces more of the liquid-liquid interfacial area than a similar rigid particle. The adsorption energy of a soft particle adsorbing into the interface from the water is the same as a similar rigid particle, if the value of γ_{2S}/γ_{12} is high. As the value of γ_{2S}/γ_{12} decreases, the adsorption energy of soft particles increases compared to rigid particles, due to the spreading of the soft particle. And when $\gamma_{1S}/\gamma_{12} + \gamma_{2S}/\gamma_{12} < 1$, the interfacial tensions are favoring total spreading of the soft particle and its adsorption energy is orders of magnitude larger than a rigid particle. There is a critical point at $\gamma_{2S}/\gamma_{12} = 0$ and $\gamma_{1S}/\gamma_{12} = 1$, where perfectly soft particles are at the edge between perfectly spreading and desorbing, and even a small change in the interfacial tension can cause the change. For example, since gel particles are swollen by the solvent, their surface properties can be also dominated by the solvent. Therefore, the interfacial tension between the gel particle and the solvent phase is small ($\gamma_{2S}/\gamma_{12} \approx 0$) and the interfacial tensions between the gel particle and the other liquid would be close to the liquid-liquid interfacial tension ($\gamma_{1S}/\gamma_{12} \approx 1$). Gel particles could be designed so that a small changes in temperature or pH (resulting in the change of interfacial tensions) could change the particle behavior from spreading to desorbing i.e. between extremely high adsorption energy and zero adsorption energy. Depending on the particles size and mechanical properties, the particle can behave as perfectly soft, perfectly rigid, or semi-soft. Semi-soft particles properties are intermediate between two extremes. If the liquid-liquid interfacial tension is not too large, then larger particles behave as rigid and smaller particles behave as perfectly soft (liquid droplets). [52]

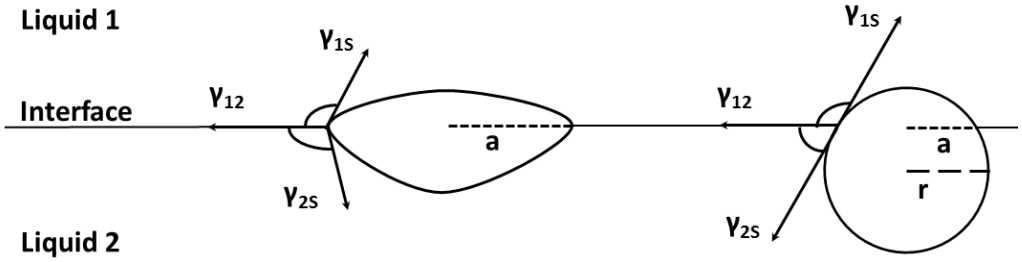

Figure 5. Deformed soft particle in comparison to a rigid particles at the liquid-liquid interface. Contact radius with the interface = a, original radius = r.

1.6 Janus particles at liquid-liquid interface

1.6.1 Spherical Janus particles

Janus particles are colloidal particles with both hydrophilic and hydrophobic regions i.e. regions with opposing wettability. In general, the equilibrium position of a colloidal particle at the liquid-liquid interface is determined by the minimization of the interfacial energy between solid and liquid phases, and between the two liquid phases. For chemically symmetric and spherical Janus particles with equal areas of hydrophobicity and hydrophilicity, the energies

are both minimized at contact angle 90° in the liquid-liquid interface, and when the interface follows the Janus boundary between hydrophobic and hydrophilic regions, so that the hydrophobic region is in the oil phase and the hydrophilic region is in the aqueous phase. In contrast, homogenous spherical particles show varying contact angles depending on their surface properties, since the interfacial energies are inversely proportional i.e. for example, minimization of interfacial energy between solid and liquid phases maximizes the interfacial energy between the two liquid phases, and therefore, the equilibrium position is found by minimizing the sum of the two energy components. For spherical chemically symmetric and moderately asymmetric Janus particles, the equilibrium position at liquid-liquid interface is generally such that the interface follows the Janus boundary (Figure 6.). The Janus boundary does not need to be at the center of the particle but it needs to be within a certain range from center called Janus regime. Highly chemically asymmetric Janus particles can behave as homogenous particles, if the ratios of the two opposite wettability are either very large or very small, then the equilibrium position is the same as for similar homogenous particle. Janus particles can be also trapped in a non-equilibrium orientation due surface roughness. The adsorption energy of a chemically symmetrical Janus particle can be approximately three times as much as the adsorption energy of a similar homogenous particle. The adsorption energy of a spherical Janus particle decreases as the chemical symmetry decreases. [50]

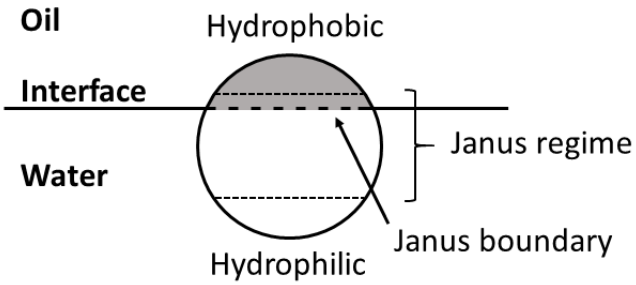

Figure 6. Janus particle at the liquid-liquid interface showing the hydrophilic and hydrophobic sides with Janus boundary and Janus regime.

1.6.2 Non-spherical Janus particles

Non-spherical homogenous particles with large aspect ratio (such as cylinders or ellipsoids) tend to adopt a horizontal orientation at the liquid-liquid interface to displace a maximum amount of the interfacial surface. But if one half of, for example, a cylinder particle is hydrophilic and the other half is hydrophobic, the geometric and chemical properties drive the particles orientation to opposite directions and the interplay between these properties determine the orientation of the particle (Figure 7.). In general, Janus ellipsoids, cylinders and dumb-bells (two opposite wettability particles fused together) adopt a vertical orientation if the wettability between the two regions is large or if the aspect ratio is close 1 i.e. the geometry is close to spherical. The Janus particle may adopt tilted orientation where the particle is not vertically nor horizontally located at the interface, if the wettability difference is low or the aspect ratio is high. [50]

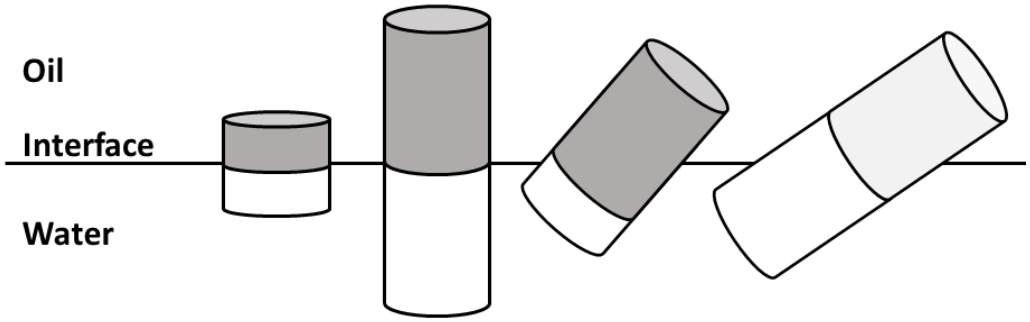

Figure 7. Janus cylinders at different orientations in the liquid-liquid interface.

1.7 Emulsions stabilized by particles

1.7.1 Size, shape, and concentration

Emulsions stabilized by particles are also called Pickering emulsions. They are named after Pickering who described the phenomena in 1907 [53]. Liquid-liquid emulsion with droplet size between 1-100 µm (macroemulsions) are thermodynamically unstable, but their degradation may be so slow that they can be considered kinetically stable, or metastable [45]. The particles ability to stabilize emulsions depends on the particle size and shape, size distribution, particle concentration, particles wettability, particle-particle interactions, and on the oil and aqueous phase properties. The particles stabilize emulsions due to the steric barrier formed at the liquid-liquid interface. [45, 46, 54] The size of the particles that can be utilized to stabilize emulsions ranges from nanometers to micrometers. Experimentally, stable emulsions have been observed with particle size 5 nm to 52 µm [49]. The size of the particle needs to be orders of magnitude smaller than the droplet, and usually smaller particles form more stable emulsions due to closer packing of the particles at the liquid-liquid interface. [45, 46] Wide particle size distribution usually decreases the emulsion stability due to unorganized adsorption on the interface [46]. Increasing the particle concentration usually decreases the droplets size and results in more stable emulsions [54]. Generally, non-spherical particles with high aspect ratio can stabilize emulsion at lower concentrations than similar spherical particles. [55] In some cases non-spherical particles can stabilize emulsion that spherical particles are unable to stabilize. [49] This is due to the higher surface area displaced at the interface resulting in larger free energy of adsorption for a disc-shaped particle compared to spherical particle of the same volume. [55, 46] Also, anisotropic particles induce greater curvature of the liquid-liquid interface that results in attractive capillary forces between particles at the interface. [49, 55] Capillary pressure is the result of the curvature of the liquid-liquid interface in between the solid particles at the interface. [45, 49] Long fiber-shaped particles can also induce greater steric barrier against coalescence due to entanglement of the fibers. The surface roughness of the particle can increase or decrease the emulsion stability. Some surface roughness can increase the capillary forces between particles and increase the emulsion stability. [46] But excessive roughness can decrease the emulsion stability due to heterogeneous wetting of the particles [46, 55].

1.7.2 Wettability

The contact angle dictates weather the oil-in-water emulsion (O/W) or water-in-oil emulsion (W/O) is more favorable assuming the oil/water volume ratio is equal to 1 [54]. If the contact angle on the aqueous phase side is < 90°, the particle is more wetted by the aqueous phase and

O/W is more favorable. And similarly, if the contact angle is > 90°, the particle is more wetted by the oil phase and W/O is more favorable. If the contact angle is very close to 90°, than no favorable emulsion type exists and the type of the emulsion depends on other factors such as solution and particle properties, and concentration of the particles. Very low (≈ 0°) or very high (≈ 180°) contact angles do not result in stable emulsions [45] as predicted by the equation of adsorption free energy. Experimentally, stable emulsions have been observed with contact angles between 20° to 120° [49]. The equation also states that the energy maximum is achieved at contact angle 90°, but the equation does not count for capillary pressures, and therefore the maximum stability of the emulsion is achieved when the particle is slightly more wetted by the continuous phase. [47, 49] Either O/W or W/O emulsions can be prepared by changing the oil/water volume ratio without altering the particle wettability. In a system consisting of particles, water, and oil, the type of emulsion can be changed by increasing, for example, the oil fraction. Initially, when the oil fraction is low, O/W emulsion is formed, but when the fraction of oil is gradually increased and reaches a critical oil/water volume ratio, phase inversion occurs and the system transitions into W/O emulsion. The exact value of the critical oil/water volume ratio depends on the particle wettability. As the hydrophilicity of the particle is increased, the value of critical oil/water ratio increases. This is since hydrophilic particles are more wetted by aqueous phase and prefer the formation of O/W emulsions. Similarly, hydrophobic particles are more wetted by the oil phase and prefer the formation of W/O emulsions, and the value of critical oil/water ratio is decreased. If the particle is well wetted by both oil and aqueous phase and it can be dispersed in either one of the phases, the value of critical oil/water volume ratio depends on in which phase the particles were dispersed before emulsification. If the particle was first dispersed in water phase, the value of critical oil/water volume ratio is high i.e. more oil than water. And if the particle was first dispersed in oil phase the value of critical oil/water volume ratio is low i.e. more water than oil. This could be explained by the different contact angles the particles adopt depending on from which phase the particle is adsorbed to the interface, which is attributed to the hysteresis of the contact angle caused by surface roughness. The contact angle is more likely to be smaller at side of the original phase i.e. particle is more wetted by the phase where it was originally dispersed. Therefore, the particles appear more hydrophilic if they were dispersed in aqueous phase prior to emulsification, and they appear more hydrophobic if they were dispersed in oil phase prior to emulsification. [54]

1.7.3 Particle-particle interactions

Since the particles are very strongly attached to the interface, the particles are more likely to move along the interface rather than to desorb into the bulk phase. Therefore, particle-particle interaction such as electrostatic repulsion, dipole-dipole repulsion, and van der Waals attractions, in addition to capillary forces are important for the structuring of the particles at the interface and the stability of the emulsion. [45] Coalescence of two bare droplets requires for the draining and thinning of the film between droplets. As the thinning progresses, a hole in the film is formed and due to its expansion the film becomes eventually unstable and coalescence takes place. If the droplets are covered with particles, they need to be dislocated for coalescence to take place. The particle are more likely to move along the interface rather than desorb due to the high adsorption energy, and therefore, particle-particle interactions may become the limiting factor in the emulsion stability. [45] The idealized arrangement of the particles at the interface is a closely packed single monolayer. This kind of ideal monolayer is not often observed due to various reasons, but the limiting factor may be the availability of dispersed particles to adsorb at the newly formed liquid-liquid interface during the emulsification process. Also, independent of particle concentration, the dispersed particles may

be in weakly-aggregated in the bulk continuous phase and are therefore unable to arrange as a closely packed monolayer. This leads to incompletely covered droplets and non-ideal arrangements of the particles at the interface. [55] Particles may have been partially-flocculated or coagulated in the bulk-phase prior to adsorption forming clusters of particles at the interface. The particles can also form chain like flocculations at the interface due to attractive capillary forces. [45] Therefore, instead of forming a monolayer, the particles are structured in the continuous phase forming a disordered multilayer of particles due to attractive particle-particle interactions [49, 55]. The multilayer exhibits gel-like structure and enhances significantly the emulsions stability against coalescence. [55] Particles can also form stable droplet flocs by bridging between droplets. This can be formed through multilayer adsorption, or if the particle concentration is low, and droplets are only partially covered with particle, in the way that the particle adsorbed at one droplet can interact with the bare surface of another droplet bridging the two droplets by a single monolayer. [45]

1.7.4 Oil and aqueous phase properties

Colloidal particles dispersed in the aqueous phase are usually charged and affected by the electrolyte concentration of the aqueous phase. Increased electrolyte concentration reduces their surface potential and leads to coagulation of particles into flocs. As the electrolyte concentration is increased, the particles become less charged due to screening of the surface charge and therefore more hydrophobic. The increased hydrophobicity of the particle results in weakly flocculated particles, which increases the emulsion stability. If the electrolyte concentration is increased further, the particles are completely flocculated, which decreases the emulsion stability. [54] Particles appear more hydrophobic at the liquid-liquid interface when the oil phase is polar, such as ester or alcohol. This results in W/O emulsion being more favorable. And when the oil phase is non-polar such as alkene, the particles appear more hydrophilic, resulting in O/W emulsion being more favorable [46, 54]. The rheological properties of the interface and continuous phase also contribute to the emulsion stability. Increased viscosity can increase the emulsion stability, due to hindering the draining and thinning of the film between droplets. [46]

1.8 Chitin, chitosan, and other selected polysaccharides

1.8.1 Polysaccharides

Polysaccharides among with proteins and nucleic acids are biopolymers produced by living organisms. Polysaccharides consist of monosaccharides that are bonded by glycosidic linkages such as starch, cellulose, chitin/chitosan, and alginate. Since all these polymers are produced by living organisms, they are renewable and biodegradable. [49] In polymeric form polysaccharides are hydrophilic and some of them, such as, starch, chitosan, and alginate, can be dissolved in aqueous solutions. Although, polysaccharides show very little interfacial activity in polymeric form due to the lack of hydrophobic moieties [56, 57, 58], in particle form polysaccharides can stabilize emulsions by adsorbing at the liquid-liquid interface [59, 60, 61]. Polysaccharide particles have found use in pharmaceutical [62, 63], food [64, 59, 65], and environmental applications [44, 43] due to their desirable properties such as, cheapness, biocompatibility, non-toxicity, and sustainability [66].

1.8.2 Chitin and Chitosan

Chitin consists of linear β(1,4)-linked *N*-acetyl-D-glucoseamine units (Figure 8.). Hydrogen bonding between adjacent monomers stabilize the linear conformation. Hydrogen bonding and van der Waals interactions between polymer chains stabilize the structure and make chitin partially crystalline. Chitin is found in fungi, and in the shells of crustacean and insects, for example. Its structure gives toughness to the shells of the crustacean and insects. Chitosan can be produced from chitin by deacetylation. This is commercially done in hot concentrated aqueous NaOH solution. Therefore, chitosan consists of β(1,4)-linked D-glucoseamine units. The degree of deacetylation (DD) can vary between 0-100%. Usually, when DD > 50% the polymer is called chitosan and when DD < 50% it's called chitin. Although, DD of 0 or 100% is practically difficult to achieve, and therefore, to be exact, both chitin and chitosan are copolymers consisting of randomly distributed β(1,4)-linked *N*-acetyl-D-glucoseamine and β(1,4)-linked D-glucoseamine units. Chitin is insoluble to common solvents, while chitosan is soluble to dilute aqueous acid solutions due to the protonation of the free primary amino groups exposed by deacetylation. The pK_a value of the amino groups is 6.5, approximately. Recently [67], novel aqueous systems have been developed to dissolve both chitin and chitosan. By varying the LiOH and KOH ratio in LiOH/KOH/urea aqueous solution, chitin and chitosan with DD values between 5 to 94% can be dissolved using freezing/thawing method.

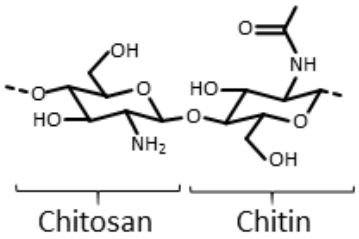

Figure 8. Structures of chitosan and chitin showing the deacetylated glucoseamine unit (chitosan) and acetylated glucoseamine unit (chitin).

1.8.3 Cellulose

Cellulose consists of linear β(1,4)-linked D-glucose units (Figure 9.). The structure is very similar to chitin and chitosan, except that the amide or amine group, respectively, is replaced by a hydroxyl group. The hydrogen bonding between adjacent glucose units stabilizes the linear configuration of the polymer chain. The interaction between polymer chains due to van der Waals forces and hydrogen bonding makes cellulose relatively stable and partially crystalline. The structure of cellulose provides stiffness to trees, plants, and algae, for example. [68] Native cellulose is insoluble in common solvents.

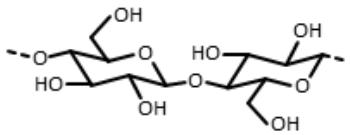

Figure 9. Structure of cellulose showing two adjacent linearly β(1,4)-linked D-glucose units.

1.8.4 Starch

Starch is a mixture of two polysaccharides, amylose and amylopectin. Amylose consists of linear α(1,4)-linked D-glucose units and it's slightly α(1,6)-branched constituting approximately 18-33% of starch. Amylopectin also consists of linear α(1,4)-linked D-glucose units but it's highly α(1,6)-branched and it constitutes approximately 72-82% of starch (Figure 10.). The exact composition depends on the source of the starch. [69] Starch can be extracted from variety of sources. Industrially the most important source is maize, and other sources being potato and wheat, for example. [70] Starch is soluble in hot water.

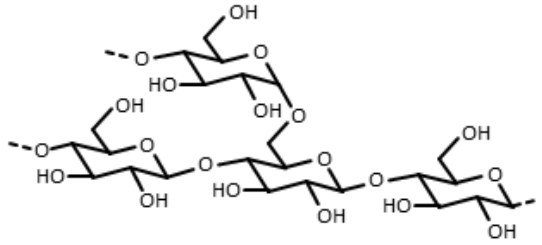

Figure 10. Structure of starch showing the linearly α(1,4)-linked D-glucose units and α(1,6)-branching.

1.8.5 Alginate

Alginate is a linear copolymer of β(1,4)-linked D-mannuronic (M) and α(1,4)-linked L-guluronic (G) acids with pK_a values 3.38 and 3.65, respectively (Figure 11.). [71] The physical properties of alginate depend on the distribution of M and G monomers and on the molecular weight. [72] Three different segments are present in the alginate: M-M, G-G, and alternating M-G segments. Sodium alginate (salt form of alginate) containing more G monomers is more soluble in water than sodium alginate containing more M monomers. Alginates can be produced from algae or bacteria but the commercially available alginates are prepared mainly from brown algae by using alkaline extraction. [73]

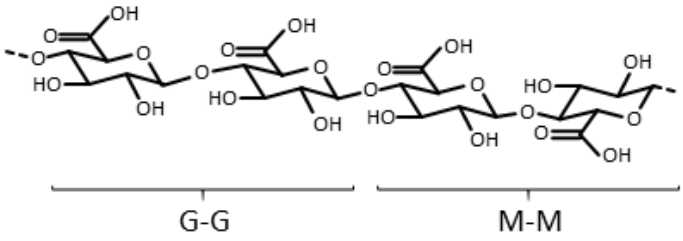

Figure 11. Structure of alginate showing the G-G and M-M segments.

1.9 Synthesis of polysaccharide nanoparticles by selected methods

1.9.1 Self-assembly methods

Amphiphilic polysaccharides can form small size micelles or aggregates in aqueous solutions, which can be exploited to produce nano and micro scale particles. The polysaccharides needs to be water-soluble and contain hydrophobic moieties, and as the polysaccharides are dissolved in water, aggregation occurs due to the interaction between the hydrophobic moieties.

Depending on the hydrophobic and hydrophilic functional groups, the properties of the particles can be adjusted. [71] The technique can be utilized to make monodisperse particles in mild conditions, but it may require heavy modification of the polysaccharides to introduce suitable hydrophobic and hydrophilic functional groups.

1.9.2 Ionic gelation of polyelectrolyte

Polyelectrolytes can be aggregated by oppositely charged multivalent ions or molecules in to small particles. The polyelectrolyte is cross-linked due to the interaction between multivalent ions and the charged functional groups in the polyelectrolyte. For example, chitosan is a positively charged polysaccharide due to the primary amino groups and alginate is a negatively charged polysaccharide due to the carboxylic groups. These polysaccharide solutions can be aggregated into small particles by addition of sodium tripolyphosphate (TPP) solution or calcium chloride solution, respectively. Ionic gelation is a simple, convenient, controllable, and aqueous phase process for nanoparticle preparation without organic solvents or toxic chemicals. [71]

1.9.3 Complex coacervation method

Similar to ionic gelation, two oppositely charged polyelectrolytes can be used to produce small particles. For example, chitosan and alginate solutions can be mixed to form aggregates due to the oppositely charged functional groups in chitosan and alginate. The method is simple aqueous phase process with mild conditions. [71] The particle size may be difficult to control and also the agglomeration of particles might be difficult to prevent. Additionally, the particles show limited stability depending on the used biopolymers. [66]

1.9.4 Desolvation/precipitation method

Polysaccharide particles can be formed by first dissolving the polymer into an aqueous solution followed by desolvation of the polymer. The desolvation can occur due to charge changes in the polysaccharide or by addition of an anti-solvent making the polysaccharide insoluble in the aqueous phase. [71] For example, the desolvation can be done by adjusting the pH until the functional groups in the polyelectrolyte are neutralized and it is no longer charged and soluble in the aqueous phase. Addition of an anti-solvent, such as an organic solvent, requires that it is miscible over the concentration range at which it will be used. The desolvation is induced by the interactions between solvent, solute and anti-solvent. The solute-solute interactions overcome the other interactions and entropy of mixing at some solvent/anti-solvent ratio, and the solute precipitates. The particles need to have sufficient particle-particle repulsion to avoid aggregation. [66] The stages of desolvation/precipitation method are: supersaturation, nucleation, particle growth, coagulation [74]. The desolvation/precipitation method is attractive due to its simplicity, cheapness, and scalability [75]. It is also widely used industrially to produce particles for pharmaceutical applications. [66]

1.9.5 Emulsification method

Polysaccharides are dissolved in water and an emulsion is formed with an immiscible phase, which can be an oil (W/O emulsion) or another aqueous phase (W/W emulsion), for example aqueous protein solution and aqueous polysaccharide solution. After the emulsification the polysaccharide is gelled inside the droplets to form small particles. More complex particle

structures can be prepared by employing W/W/O or W/O/W emulsions. The prepared particles need to be separated from the oil phase by centrifugation, filtering, and/or washing. [66] Due to the more complex reaction conditions and the use of large amounts of organic solvents, the emulsification method has some drawbacks compared to aqueous phase methods. The conventional emulsification method has been further developed by employing microfluidic devises or membranes to prepare small droplet W/O emulsions. [71]

1.9.6 Isolation of nanocrystals

Many of the polysaccharides are semi-crystalline and the crystalline phase can be extracted from the amorphous phase by variety of methods to yield nanocrystals. For example, cellulose [61], chitin [76, 77], and starch [59] nanocrystals have been prepared using acid hydrolysis and the resulted nanocrystals have been employed to stabilize emulsion. In acid hydrolysis, typically either HCl or H_2SO_4 aqueous solutions are used with the solid polysaccharide dispersed in the solution. The reaction is allowed to proceed for hours or days depending on the raw material, polysaccharide, and reaction parameters, such as acid concentration, acid type, and temperature [70, 78]. The amorphous phase is hydrolyzed into soluble species and dissolved while the solid crystalline phase is left intact. Nanocrystals and nanofibers of α-chitin and cellulose can be also isolated by 2,2,6,6-tetramethyl-piperidinyl-1-oxyl (TEMPO)-oxidation. The chitin or cellulose is dispersed in alkaline (pH 10) aqueous solution containing TEMPO and NaBr, and the oxidation is initiated by addition of NaOCl as co-oxidant. During the oxidation, the amorphous phase is dissolved. Some of the hydroxyl groups in α-chitin crystals are transformed into carboxyl groups, which induce negative electric repulsion between nanocrystals inhibiting their agglomeration. Chitin is not deacetylated during TEMPO-oxidation. Another way to prepare chitin nanofibers is partial deacetylation of chitin followed by mechanical disintegration into nanofibers. This method produces nanofibers with positive surface charge due to deacetylation and formation of free amino groups, in contrast to the negatively charged nanofibers produced by the TEMPO-oxidation.

1.10 Chitosan nanoparticles

1.10.1 Synthesis of chitosan nanoparticles

Native chitosan nanoparticles can be prepared by desolvation without cross-linking agents by simply adjusting the pH close to the pK_a value (≈ 6.5) of the amino groups [79, 80]. Ultrasonication may be used to assist the dispersing of the chitosan particles into the solution [81, 82]. The amino groups can be also exploited to synthesize nanoparticles using ionic or covalent cross-linking. Ionic cross-linking with tripolyphosphate (TPP) has received a lot of attention in the literature due to its applications in drug delivery systems [83, 84] and the different parameters affecting the formation and properties of the nanoparticles has been thoroughly explored [85, 86, 87]. The synthesis is simple, first the chitosan is dissolved in dilute aqueous acid solution. Acetic acid is widely used in literature to dissolve chitosan. And second, the TPP solution is added into the chitosan solution while stirring. The negatively charged multivalent polyphosphate anion attracts the positively charged amino groups in chitosan and cross-links the polymer chains to form particles. For the formation of nanoparticles, the maximum concentrations of TPP and chitosan are 1.0 mg/ml and 1.5 mg/ml, respectively. Generally, the particle size increases as a function of the concentration of either TPP or chitosan. Also, as the mass ratio of chitosan to TPP decreases, the size of the particles also decreases due to the increased cross-linking density. The effect of pH was also studied

from 3.6 to 5.5, and it was concluded that the optimal chitosan to TPP mass ratio decreased with decreasing pH, mainly due to the changes in the protonation degree of the amino groups in chitosan. The particle size decreased with increasing temperature from 10-60 °C which was attributed to the decrease in the viscosity of the chitosan solution. Increased stirring speed was found to decrease the particle size distribution between 200 to 800 rpm but higher stirring speed caused also small amount of aggregation of the particle. [85] Due to the simplicity of the synthesis, it has been studied for scale-up [88, 89, 90] using different kind of static mixers to produce the nanoparticles continuously. An example of covalent cross-linking of chitosan is using glutaraldehyde as the cross-linking agent. The aldehyde groups in glutaraldehyde react readily with the primary amino groups of chitosan producing an imine. Emulsification method usually employed to prepare glutaraldehyde cross-linked chitosan particles. A water-in-oil emulsion is prepared using the aqueous chitosan solution and glutaraldehyde is added into the emulsion [91].

1.10.2 Chitosan nanoparticles at liquid-liquid interface

Native chitosan nanoparticles were prepared by adjusting the pH to 6.5-6.9 [79, 82, 81] and oil-in-water emulsions stabilized by the prepared particles were studied. The particle could form stable emulsion by adsorbing into the liquid-liquid interface with at least liquid paraffin, n-hexane, toluene, dichloromethane, [79] corn oil, [82] palm oil, [81] and medium chain triglycerides [80] which have varying properties, such as dielectric constants and viscosities. Liu et al. [79] demonstrated reversible emulsification of liquid paraffin by exploiting the reversible formation of the particle by pH adjustment. The emulsion could be formed by mixing the aqueous particle dispersion with oil and then demulsified by adding HCl to dissolve the particles. The particles could be reformed by adjusting the pH back to 6.7 and the emulsion could be reproduced. The recycling could be done at least 5 times. Mwangi et al. [80] studied the effect of chitosan concentration, ionic strength, pH, and temperature on the stability of medium chain triglycerides emulsions stabilized by chitosan particles. The droplets diameter was inversely proportional to the chitosan concentration indicating that increasing the amount of particles decreases the droplet diameter due to the more available particles to adsorb into the interface. The influence of NaCl concentration was studied between 0-500 mM and coalescence and creaming stability were improved on all NaCl concentrations. This was attributed to the decreased repulsions between adsorbed and non-adsorbed particles and resulting enhancement of the interfacial film. The increase of pH to 7-8 increased the stability of the emulsions due to the aggregation of the particle around the droplets resulting in strengthening of the interfacial film. When the pH was decreased from 6 to 3, an increase in the droplet diameter was observed due to the partial dissolution of the particles, and in pH 2 demulsification occurred. The effect of temperature (30-90 °C) was studied with 30 min heating time. The emulsions were stable up to 50 °C after which droplet size increased significantly, which was attributed to increased Brownian motion of the particles.
Chitosan nanoparticles cross-linked with TPP were applied to stabilize medium chain triglyceride in water emulsion and the stability of the emulsions were studied as a function of time, pH, and ionic strength. The higher chitosan concentration increased the emulsion stability during the storage time. In low concentration samples the droplet size increased while higher concentration samples remained almost unchanged. The effect of pH was not significant between pH values 2-7. The droplets sizes remained nearly constant at pH 2-4 but slight increase in pH 5-7 was observed. This was attributed to the low charge at the surface of the droplets resulting in only weak repulsion. [92] Alternatively, this could be explained by the degradation of the particles due to the deprotonation of the amino groups at near neutral pH. The effect of salinity (NaCl or $CaCl_2$) was also studied at concentrations 0-200 mM in pH 3,

6, and 7. The addition of salt into the emulsions did not change the emulsions significantly but a slight increase in droplet size was observed [92].

1.11 Carboxymethyl chitosan

1.11.1 Properties of carboxymethyl chitosan

The applications of chitosan are limited by its solubility in only acidic aqueous solutions. Chitosan can be made soluble in neutral and alkaline aqueous solutions by introducing carboxylic groups into chitosan. Due to the presence of both amino and carboxylic groups, the solubility of the carboxymethyl chitosan differs from the native chitosan. The pKa of the carboxylic groups is approximately 4 and since there is also amino groups present in the polymer back-bonce, there is an isoelectric point at approximately pH 5. The isoelectric point results in insolubility of the polymer at around pH 5 due to the strong attraction between oppositely charged amino and carboxylic groups. The carboxymethyl chitosan is soluble at pH ≤ 3 and ≥ 7, approximately. The exact pH range of insolubility depends on the reaction conditions, such as temperature. [93] Carboxyl modified chitosan is a widely studied chitosan derivative due to its simple preparation, non-toxicity, and biodegradability [94].

1.11.2 Synthesis by reductive alkylation using aldehydes

The primary amino group in chitosan is reacted with glyoxylic acid to form an imine. The imine is reduced to give *N*-Carboxymethyl chitosan by using a reducing agent, such as $NaBH_4$ or $NaCNBH_3$. The reaction can be done in homogenous conditions due to the solubility of chitosan in dilute acidic aqueous solutions. The reaction is selective to amino groups leaving hydroxyl groups unreacted. Although, disubstituted *N*,*N*-Carboxymethyl chitosan is also formed due to the high reactivity of glyoxylic acid. The substitution degree of *N*-Carboxymethyl chitosan can be controlled by varying the relative amounts of reagents and reaction conditions. Reductive alkylation requires fairly expensive reagents such as, glyoxylic acid, $NaBH_4$, and $NaCNBH_3$ making it an expensive process to prepare carboxymethyl chitosan. [95, 96]

1.11.3 Synthesis by direct alkylation using monochloroacetic acid

The hydroxyl and/or amino groups of chitosan are reacted with monochloroacetic acid in heterogeneous conditions in a mixture of water, isopropanol, and NaOH. By varying the reaction conditions, *N*-carboxymethyl, *N*,*O*-carboxymethyl, or *O*-carboxymethyl chitosan can be prepared. Highly alkaline conditions and low temperature (approximately 50% NaOH) favors the formation of *O*-carboxymethyl chitosan. Lower alkalinity and higher temperature also allows the reaction of amino groups and results in *N*,*O*-carboxymethyl chitosan. Deacetylation and depolymerization of the native chitosan also occurs during the reaction due to very high NaOH concentrations. [93, 97]

1.12 Carboxymethyl chitosan nanoparticles

Carboxymethyl chitosan nanoparticles can be synthesized with similar strategy as chitosan nanoparticles. Due to the presence of carboxylic groups, it is possible to use positive multivalent ions to ionically cross-link the polymer chains. For example, calcium ions can be used for this purpose [98, 99, 94]. The negatively charged carboxylic groups at pH ≥ 7 can

interact with the positively charged Ca^{2+} ions and cross-link the polymer chains to form particles. This has certain advantages that the native chitosan nanoparticles cross-linked with TPP do not have, such as the ability to prepare nanoparticles at neutral and alkaline pH. The native chitosan nanoparticles aggregate at neutral or higher pH due to the deprotonation of the amino groups and subsequent degradation of the nanoparticles due to lack of cross-linking. In the literature, the calcium cross-linked carboxymethyl chitosan nanoparticles are mainly studied for encapsulation and controlled-release of substances [100, 101, 99, 102, 103, 98]

Shi et al. [98] determined the effect of carboxymethyl chitosan and $CaCl_2$ concentration, and carboxymethyl chitosan molecular weight and substitution degree, to the formation of carboxymethyl chitosan nanoparticles. The particle size and size distribution increased as the concentration of either carboxymethyl chitosan or $CaCl_2$ was increased. Increasing molecular weight of the carboxymethyl chitosan decreased the amount of calcium ions required to form nanoparticles. This was attributed to the conformational changes of longer chain carboxymethyl chitosan during the coordination to calcium ions. Also, increased substitution degree decreased the amount of required calcium ions, which was attributed to the increased negative charge density in the highly substituted carboxymethyl chitosan. [98] Although, alternatively both of these trends can be explained by the increased cross-linking between polymer chains, which leads to the formation of insoluble aggregates i.e. nanoparticles. Longer polymer chains requires less calcium ions to cross-link the same weight of the carboxymethyl chitosan. In addition, the solubility of polymers usually decreases as the molecular weight increases, which could contribute to the aggregation of the longer chain carboxymethyl chitosan. Higher substitution degree also increases the cross-linking between polymer chains due to the increased probability of inter chain cross-linking rather than intra chain cross-linking. Shi et al. [98] also reported that increased molecular weight increased the size of the nanoparticles due to entanglement of the longer polymer chains, and the increase in substitution degree decreased the size slightly due to more compact conformation of the polymer chains. The effect of pH was not studied by Shi et al. or any other author in the literature. Also, carboxymethyl chitosan nanoparticles have not been studied for their emulsification properties. Although, it has been noted recently that they could have potential in the field of Pickering emulsions [104].

2 Research objectives

The objective of this research work was to develop chitosan-based nanoparticles for possible use in oil-spill treatment. The particles should adsorb into the liquid-liquid interface and stabilize oil-in-water emulsions. The emulsification of oil could prevent the oil from spreading on the water surface and also increase the surface area of the oil and make it more available to the natural biodegradation. For effective adsorption into the liquid-liquid interface, the particles need to be well dispersed in the aqueous phase. Therefore, colloidal particles (1-1000 nm) would be most suitable for this purpose. Both the adsorption free energy and the size of the stabilized droplet increases with the increase of particle size. Therefore, to maximize the emulsion stability, the particle size should not be very small (≈ 1 nm) but not very large (≈ 1000 nm) since the droplet size is generally inversely proportional to the emulsions stability. Most of the water in nature is sea water with pH of approximately 8 and the salinity of up to 3.5m-%. The chitosan was modified to form stable colloidal particles in pH ≥ 7, since native chitosan is insoluble and neutral at pH > 6.5. Since carboxymethyl chitosan nanoparticles have not been studied previously as emulsifiers and they are capable of forming stable nanoparticles in pH ≥ 7, the research is concentrated on carboxymethyl chitosan nanoparticles and their properties.

The objectives of the study are:

Develop chitosan-based nanoparticle that are stable in pH ≥ 7 (Paper I &II).
Study the emulsification properties of the developed particles (Papers I & III)
Study reversibility of the emulsification (Paper III).
Study the effect of further modification of the particles to the emulsification properties (Papers III & IV).

3 Materials and methods

3.1 Synthesis of chitosan derivatives and their nanoparticles

3.1.1 Carboxymethyl chitosan

The carboxymethyl chitosan was synthesized using chloroacetic acid in alkaline reaction medium due to the simple reaction conditions and cheap reactants. Typically, solid chitosan (1 g) was mixed with NaOH (1.35 g), water (6 ml), and 2-propanol (24 ml). The mixture was stirred at 50 °C for 1 hour, after which chloroacetic acid (1.5 g) dissolved in 2-propanol (2 ml) was added drop wise, and the stirring was continued for 4 hours at 50 °C. The solid product was washed with 70% aqueous ethanol solution followed by washing with absolute ethanol. The product was dried at room temperature over-night.
Carboxymethyl chitosan nanoparticles were synthesized by ionic gelation and desolvation methods. Carboxymethyl chitosan was dissolved into water (0.5 mg/ml) and aqueous $CaCl_2$ solution (1.5 m-%) was added while stirring to cross-link the carboxymethyl chitosan into nanoparticles. The amount of $CaCl_2$ solution required for the nanoparticle formation depends on the pH of the aqueous phase in neutral or alkaline conditions (II). At acidic pH, the nanoparticles self-assemble due to the protonation of the amino groups resulting in attractive interaction between amino and carboxyl groups, and $CaCl_2$ solution is not needed for cross-linking (II, III).

3.1.2 Hydrophobically modified carboxymethyl chitosan

The introduction of hydrophobic moieties to carboxymethyl chitosan was done using reductive alkylation by employing aldehydes. Typically, the carboxymethyl chitosan (0.75 g) was dissolved in water (42 ml) and ethanol (30 ml) was added. Then, dodecanal (30 µl) was added and the mixture was stirred for 20 min followed by the addition of $NaCNBH_3$ (30 mg). The reaction was allowed to proceed for 20 h and then the product was precipitated in absolute ethanol (400 ml). The product was washed with 90% aqueous ethanol followed by washing with absolute ethanol. The product was dried in room temperature over-night.
Hydrophobically modified carboxymethyl chitosan nanoparticles were synthesized by desolvation method similarly to the carboxymethyl chitosan nanoparticles by adjusting the pH of the solution.

3.1.3 Vanillin-chitosan

The vanillin-chitosan was prepared by forming an imine bond between vanillin and chitosan followed by reduction of the imine into amine. Typically, chitosan solution (2%) was prepared by dissolving chitosan into aqueous acetic acid solution (1%). The vanillin (1 equivalent to available amino groups) was dissolved in acetone and added drop wise into the chitosan solution while stirring. The resulted yellow viscous solution was poured into silicon molds and dried at 70 °C for 8 hours. The formed films were ground into a fine powder (≤ 150 µm) and dispersed into an aqueous NaOH solution (0.1 M) containing $NaBH_4$ (2 equivalents to available amino groups) and stirred over-night. The solid product was washed with NaOH (0.1 M), dispersed into water (50 ml), and neutralized with HCl (1 M). The solid product was further washed with water and absolute ethanol, and dried at room temperature.
Vanillin-chitosan nanoparticles were synthesized by desolvation method. The vanillin-chitosan was dissolved in aqueous HCl (0.05 M) and the vanillin-chitosan solution was added drop wise into aqueous NaOH (0.1 M) while vigorously stirring. The nanoparticles were formed by desolvation of the vanillin-chitosan in alkaline conditions, and the colloid was stabilized by the electrostatic repulsion between the particles induced by the deprotonation of the phenol groups.

3.2 Characterizations

Fourier transformation infrared spectroscopy (FTIR) was conducted with Nicolet Nexus 8700 (USA). Dynamic light scattering (DLS) and zeta-potential measurements were conducted with ZetaSizer Nano ZS apparatus (Malvern Instruments Ltd.). Scanning electron microscopy (SEM) imaging was conducted on a Hitachi S-4800 FEG Cryo-SEM operated at 3.0 kV. Samples were allowed to dry in room temperature and the dried samples were carbon coated twice for 9.9 s with Cressington 208 Turbo Carbon Coater at 4 kV in vacuum (10−4 mbar). Transmission electron microscopy (TEM) was conducted on a FEI Tecnai G2 F30 FEG TEM operated at 200 kV and Hitachi 7700. X-ray energy dispersive spectroscopy (EDS) was conducted on Bruker AXS Microanalysis GmbH operated at 200 kV. Cryo-scanning electron microscopy (Cryo-SEM) imaging was conducted on a Hitachi S-4800 FEG Cryo-SEM operated at 3.0 kV at −120 °C. A droplet of the emulsion was frozen in slushed liquid nitrogen followed by fracturing at −130 °C. The solvent was sublimated at −95 °C for 5 min and the sample was sputtered with Pt-Pd composite at 10 mA for 88 s. Deacetylation degree (DA) of chitosan and substitution degree (DS) of carboxymethyl chitosan was determined by conductometric and potentiometric titrations by dissolving the sample in HCl or NaOH aqueous solutions and titrating with NaOH or HCl aqueous solutions, respectively. The conductance and pH of the solutions were measured and the DA and DS were determined based

on the detected inflection points. For ^{1}H NMR analyses, the samples were dissolved in D_2O containing 0.7% of DCl and placed in 5 mm NMR tubes. The ^{1}H NMR spectra were recorded using Bruker Ascend 400 MHz spectrometer and standard proton parameters with the delay time (d1) of 6 s at 70 °C.

4 Results and discussion

4.1 Carboxymethyl chitosan nanoparticles and their properties

Carboxymethyl chitosan nanoparticles were synthesized by ionic gelation method using $MgCl_2$, $CaCl_2$, and $SrCl_2$ in pH 7. Due to the weak interaction between carboxyl groups and Mg^{2+} and Sr^{2+} ions, these particles were very unstable and were not studied in detail. Nanoparticle cross-linked with Ca^{2+} (CMC-Ca) were more stable and therefore studied in more detail (Figure 12.). The CMC-Ca were fairly stable in increased salinity (up to 4m-% NaCl) at pH 7 and only the size of the particles was increased as detected by DLS measurements. The increased size could be due to the swelling of the particles in saline solution. The CMC-Ca were unstable in increased pH and larger aggregates were formed (Paper I).

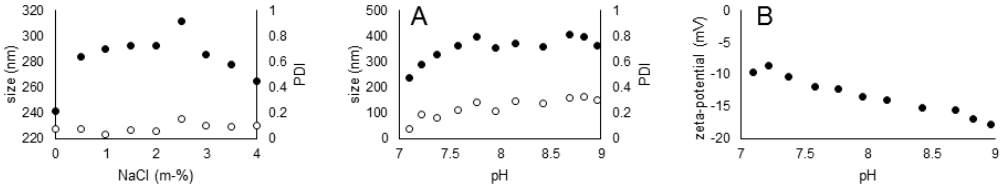

Figure 12. The size (●), PDI (○), and zeta-potential (●) of CMC-Ca nanoparticles as a function of NaCl concentration and pH. (Paper I)

The pH stability of the CMC-Ca was studied in more detail (Paper II) since at pH 7-9 all the carboxyl groups are deprotonated and the adjustment of pH should not have significant effect on the interaction between Ca^{2+} and carboxyl groups. It was found that the interaction between the protonated amino groups and deprotonated carboxyl groups in carboxymethyl chitosan had significant contribution to the stability of the particles. The CMC-Ca could be made stable in varying pH conditions (7-9) by adjusting the pH to the desired value during the synthesis of the particles (Figure 13.). Simultaneously, the amount of added Ca^{2+} ions had to be increased due to the decreased interaction between protonated amino groups and deprotonated carboxyl groups. Previously in literature, the need for increased Ca^{2+} concentration was attributed to zeta-potential, hydrophobic interactions, and rigidity of the polymer chain [102]. By adjusting the pH and Ca^{2+} concentration during the synthesis, the size of the particles could be adjusted between 150-300 nm, approximately (Figure 13.). The carboxymethyl chitosan nanoparticles could be also prepared solely by the interaction between amino and carboxyl groups by decreasing the pH of the solution to approximately 6. (Paper II)

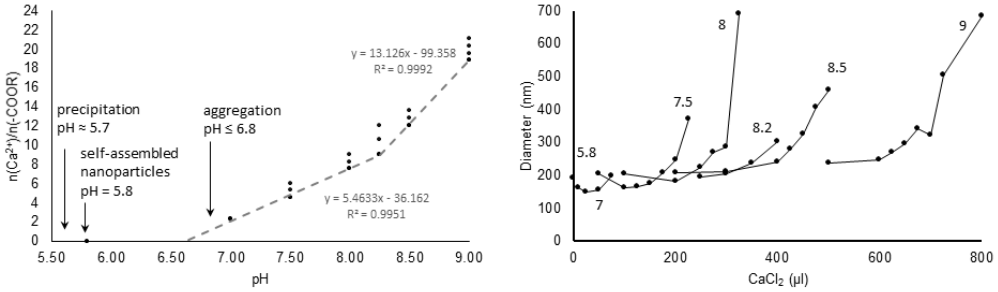

Figure 13. The formation of CMC nanoparticles as a function of Ca^{2+} concentration and pH. (Paper II)

Vanillin substituted chitosan (V-Chitosan) particles were prepared by precipitation in NaOH aqueous solution. The colloidal particles were stable in pH ≥ 10.5 due to the electrostatic repulsion induced by deprotonated phenol groups in the vanillin moieties. The size of the prepared particles were between 250-500 nm depending on the concentration of the prepared colloidal solution (Figure 14.). (Paper IV)

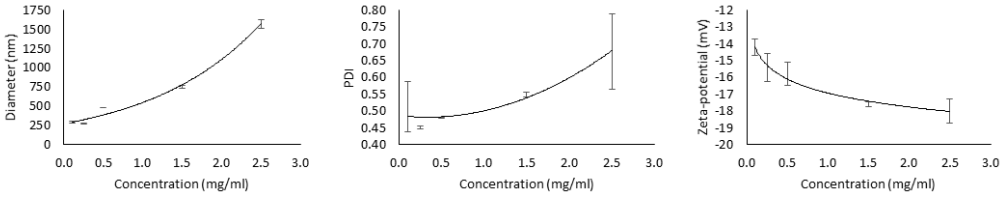

Figure 14. The size, PDI, and zeta-potential of V-Chitosan particles as a function of V-Chitosan concentration. (Paper IV)

4.2 Carboxymethyl chitosan nanoparticles in contact with liquid-liquid interface

The CMC-Ca adsorbed at the oil-water interface and could stabilize emulsions (Figure 15). The emulsion stability was improved compared to the native carboxymethyl chitosan. The CMC-Ca were detected at the oil-water interface by Cryo-SEM imaging. In comparison, native carboxymethyl chitosan was not detected at the interface and remained in the solution providing mainly steric barrier against droplet coalescence. (Paper I)

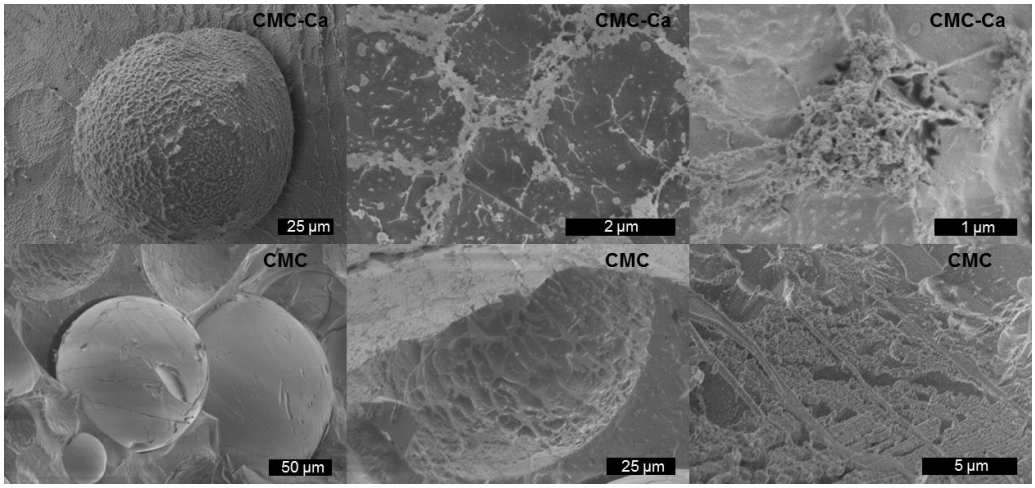

Figure 15. Cryo-SEM images of an oil droplet emulsified by CMC-Ca nanoparticles and polymeric CMC. (Paper I)

The CMC nanoparticles formed through the interaction between amino and carboxyl groups by pH adjustment formed gel-like emulsions indicating significant particle-particle interaction and bridging of the droplets. The gel-like emulsions were attributed to the inter-particle interactions between amino and carboxyl groups. Since the particle formation requires only pH adjustment, the formation and subsequent emulsification of oil could be reversed by adjusting pH (Figure 16.). The particles can be formed at low pH and the emulsion can be prepared by mixing in the presence of oil. The emulsion can be degraded and the oil returned back to liquid form by dissolving the particles in high pH. Hydrophobically modified CMC (h-CMC) containing long linear alkyl group was also synthesized, and they could attach to the oil-water interface. The h-CMC behave very similarly to CMC, except when the particles were dissolved to degrade the emulsion. At this stage, the h-CMC remained attached to the oil-water interface and the emulsion transitioned from a gel-like to free-flowing. When the pH was adjusted back to low value to reform the nanoparticle, the oil returned back to liquid state. (Paper III) In the literature, similar results have been reported for native chitosan nanoparticle prepared solely by pH adjustment, but no droplet bridging was reported [82, 79]. This may be explained by the weak interaction between native chitosan nanoparticles that are held together by hydrophobic interaction, for example. The CMC nanoparticles have oppositely charged groups that provide stronger interaction and could also contribute to the particle-particle interaction.

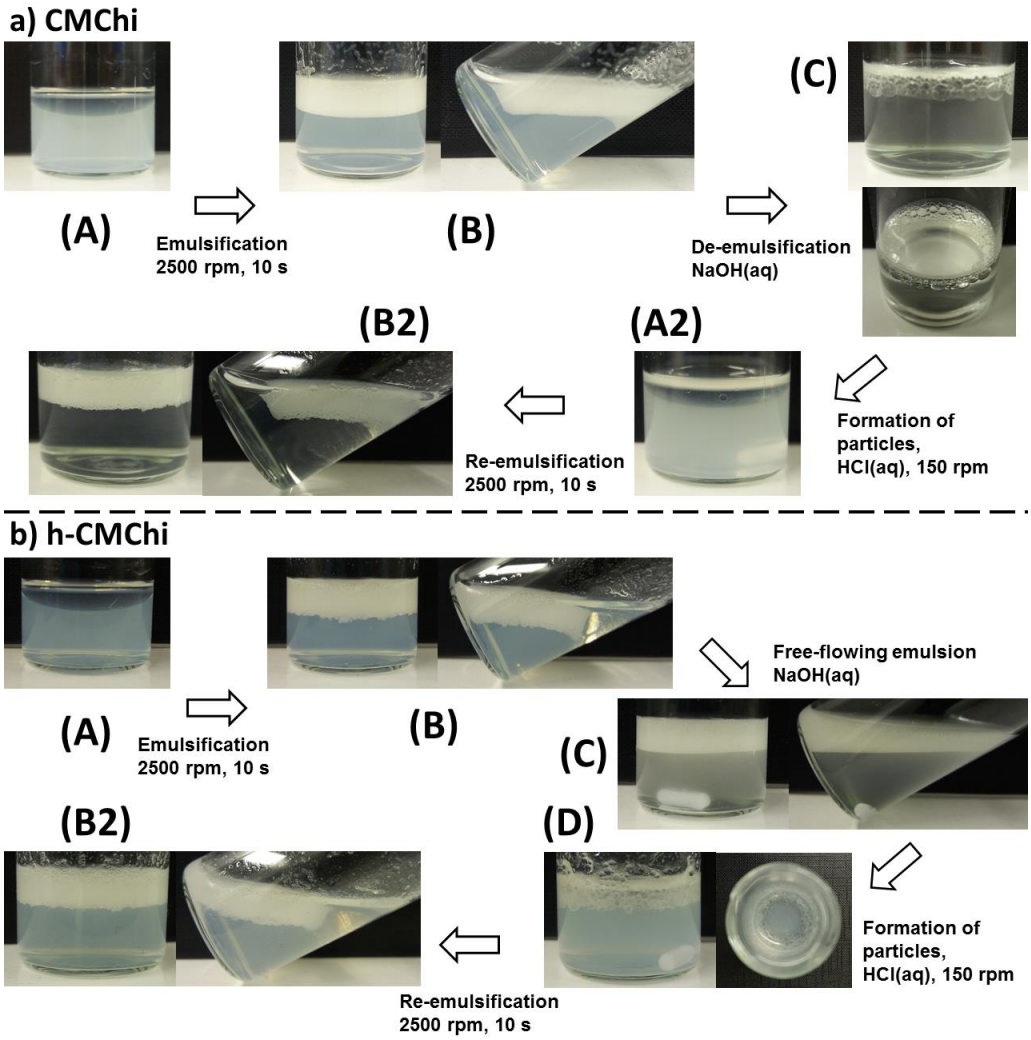

Figure 16. Reversible emulsification of oil by pH adjustment using CMChi and h-CMChi nanoparticles. (Paper III)

V-Chitosan particles formed large aggregates while mixing in contact with oil (Figure 17.). The aggregates entrapped oil droplets allowing for easier removal of oil from the water surface. The amount of immobilized oil reduced as the mixing time was increased to more than 30 s. Also, the droplet size and size distribution decreased indicating that the smaller droplets remain immobilized inside the aggregates while bigger droplets are released and coalescence (Figure 18.). The aggregation of V-Chitosan particles was attributed to the neutralization of the surface phenol groups due to the adsorption of the particles at the oil-water interface. Further, stabilization might be due to the deformation of the inherently soft polymeric V-Chitosan particles at the oil-water interface. (Paper IV)

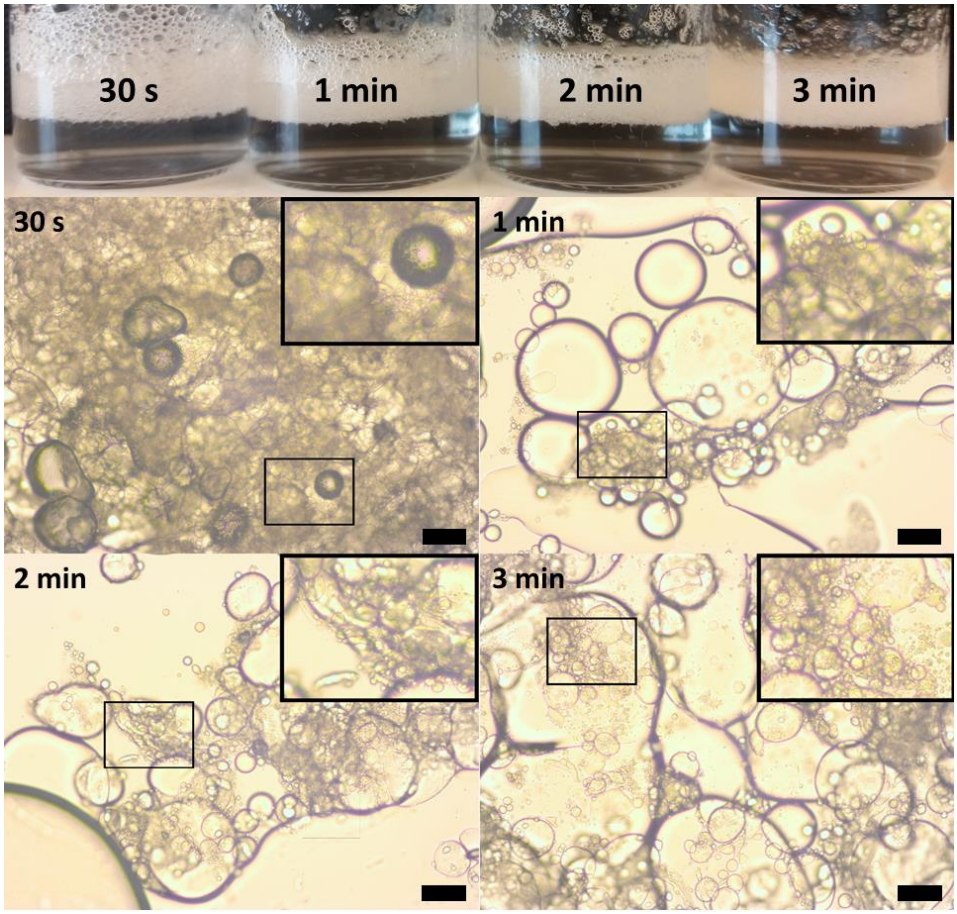

Figure 17. Oil emulsified using V-Chitosan particles. Microscope images show the encapsulation of small oil droplets inside V-Chitosan aggregates. Scale bar is 10 µm. (Paper IV)

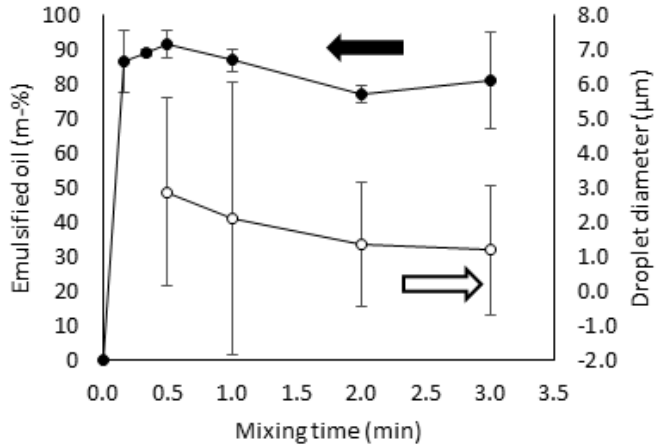

Figure 18. Emulsification of oil by V-Chitosan particles and the average droplet size as a function of mixing time (2500 rpm). (Paper IV)

5 Conclusion and further research

Chitosan is a versatile and abundant bio-based material with many desirable properties such biodegradability, non-toxicity, and renewability. The reactive amino and hydroxyl functional groups can be exploited to further modify the properties of chitosan. The introduction of carboxyl groups opens a wide range of properties due to the presence of both basic amino and acidic carboxyl groups. The functional groups of carboxymethyl chitosan provide variety of ways to prepare colloidal particles. Here, the particles were prepared by ionic cross-linking using Ca^{2+} ions and desolvation by adjusting the pH of the carboxymethyl chitosan solution. The calcium cross-linked particles were found to fairly stable in increased salinity (up to 3.5m-%) and the stability in alkaline pH (7-9) could be increased by adjusting the pH during the synthesis of the particles. Both ionically cross-linked and desolvated particles could be applied to stabilize emulsions by adsorption into the liquid-liquid interface providing greater stability compared to the native carboxymethyl chitosan. Due to the reversibility of the desolvation of the particles it was possible to reversibly emulsify and demulsify oils by simple pH adjustment. The particles could be dissolved by increasing the pH resulting in degradation of the emulsion, and then the particles could be reformed by decreasing the pH allowing for the re-emulsification of the oil. Amino (and hydroxyl) groups of chitosan can be used to further modify the properties of chitosan, for example, the hydrophilic-hydrophobic properties by introducing hydrophobic moieties like demonstrated here. Hydrophobic moieties enhanced the particles ability to emulsify oils through the attachment of the long alkyl chains into the liquid-liquid interface. The grafting of vanillin into the chitosan allowed the formation of colloidal particles at alkaline pH ($\geq$ 11). The prepared particles aggregated upon contact with oil and encapsulated small oil droplets.

Further research could focus on the development of chitosan nanomaterials with enhanced properties. The challenge is to find the suitable modifications and prepare the materials in an environmentally friendly and economical way while still retaining the desirable properties of native chitosan, such as biodegradability and non-toxicity. Efficient modification of chitosan usually requires the dissolution of the polymer. Traditionally, chitosan has been dissolved in dilute aqueous acid but the solubility of chitosan is fairly low and the aqueous and acidic reaction medium restricts some modifications. Recently, new green solvent systems for chitosan have been developed which could advance the way chitosan is processed to novel materials. On the other hand, solid-state reactions could avoid the use of solvents in the first place and in some cases could provide alternative ways to process chitosan. For example, recently the deacetylation of chitin to produce chitosan has been done as a solid-state reaction without solvents. The chitosan nanomaterials and their properties in contact with liquid-liquid interface could be studied in more detail, such as the mechanical and surface charge properties of the particles at the liquid-liquid interface. The nanomaterials structure-properties relations could guide the development of novel materials for applications in the liquid-liquid interface.

6 References

[1] C. Stevens, L. Thibodeaux, E. Overton, K. Valsaraj, K. Nandakumar, A. Rao and N. Walker, "Sea Surface Oil Slick Light Component Vaporization and Heavy Residue Sinking: Binary Mixture Theory and Experimental Proof of Concept," *Environmental Engineering Science,* vol. 32, pp. 694-702, 2015.

[2] M. Ha, H. Kwon, H.-K. Cheong, S. Lim, S. Yoo, E.-J. Kim, S. Park, J. Lee and B. Chung, "Urinary metabolites before and after cleanup and subjective symptoms in volunteer participants in cleanup of the Hebei Spirit oil spill," *Science of The Total Environment,* vol. 429, pp. 167-173, 2012.

[3] D. Dave and A. Ghaly, "Remediation Technologies for Marine Oil Spills: A Critical Review and Comparative Analysis," *American Journal of Environmental Sciences,* vol. 7, pp. 423-440, 2011.

[4] D. Prendergast and P. Gschwend, "Assessing the performance and cost of oil spill remediation," *Journal of Cleaner Production,* vol. 78, pp. 233-242, 2014.

[5] Q. Shi, D. Hou, K. Chung, C. Xu, S. Zhao and Y. Zhang, "Characterization of Heteroatom Compounds in a Crude Oil and Its Saturates, Aromatics, Resins, and Asphaltenes (SARA) and Non-basic Nitrogen Fractions Analyzed by Negative-Ion Electrospray Ionization Fourier Transform Ion Cyclotron Resonance Mass Spectrome," *Energy Fuels,* vol. 24, p. 2545–2553, 2010.

[6] M. Alexander, N. Engel, N. Olaiya, L. Wang, J. Barrett, L. Weems, E. Schwartz and J. Rusiecki, "The deepwater horizon oil spill coast guard cohort study: A cross-sectional study of acute respiratory health symptoms," *Environmental Research,* vol. 162, pp. 196-202, 2018.

[7] S. Chang, J. Stone, K. Demes and M. Piscitelli, "Consequences of oil spills: a review and framework for informing planning," *Ecology and Society,* vol. 19, p. 26, 2014.

[8] Y.-Z. Liu, A. Roy-Engel, M. Baddoo, E. Flemington, G. Wang and H. Wang, "The impact of oil spill to lung health—Insights from an RNA-seq study of human airway epithelial cells," *Gene,* vol. 578, pp. 38-51, 2016.

[9] L. Camus and M. Smit, "Environmental effects of Arctic oil spills and spill response technologies, introduction to a 5 year joint industry effort," *Marine Environmental Research,* p. In Press, 2018.

[10] S. Røberg, S. Stormo and B. Landfald, "Persistence and biodegradation of kerosene in high-arctic intertidal sediment," *Marine Environmental Research,* vol. 64, pp. 417-428, 2007.

[11] F. Motta, S. Stoyanov and J. Soares, "Application of solidifiers for oil spill containment: A review," *Chemosphere,* vol. 194, pp. 837-846, 2018.

[12] B. Doshi, M. Sillanpää and S. Kalliola, "A review on Bio-based materials for the oil-spill treatment," *Water Research,* p. in Press, 2018.

[13] R. Atlas, "Petroleum biodegradation and oil spill bioremediation," *Marine Pollution Bulletin,* vol. 31, pp. 178-182, 1995.

[14] M. Zahed, H. Aziz, M. Isa and L. Mohajeri, "Effect of Initial Oil Concentration and Dispersant on Crude Oil Biodegradation in Contaminated Seawater," *Bulletin of Environmental Contamination and Toxicology,* vol. 84, p. 438–442, 2010.

[15] S.-Z. Yang, H.-J. Jin, Z. Wei, R.-X. He, Y.-J. Ji, X.-M. Li and S.-P. Yu, "Bioremediation of Oil Spills in Cold Environments: A Review," *Pedosphere,* vol. 19, pp. 371-381, 2009.

[16] R. Garrett, S. Rothenburger and R. Prince, "Biodegradation of Fuel Oil Under Laboratory and Arctic Marine Conditions," *Spill Science & Technology Bulletin,* vol. 8, pp. 297-302, 2003.

[17] Z. Xue, Y. Cao, N. Liu, L. Feng and L. Jiang, "Special wettable materials for oil/water separation," *J. Mater. Chem. A,* vol. 2, pp. 2445-2460, 2014.

[18] Y. Cao, X. Zhang, L. Tao, K. Li, Z. Xue, L. Feng and Y. Wei, "Mussel-Inspired Chemistry and Michael Addition Reaction for Efficient Oil/Water Separation," *ACS Appl. Mater. Interfaces,* vol. 5, p. 4438–4442, 2013.

[19] X. Zhou, Z. Zhang, X. Xu, F. Guo, X. Zhu, X. Men and B. Ge, "Robust and Durable Superhydrophobic Cotton Fabrics for Oil/Water Separation," *ACS Appl. Mater. Interfaces,* vol. 5, p. 7208–7214, 2013.

[20] D. Deng, D. Prendergast, J. MacFarlane, R. Bagatin, F. Stellacci and P. Gschwend, "Hydrophobic Meshes for Oil Spill Recovery Devices," *ACS Appl. Mater. Interfaces,* vol. 5, p. 774–781, 2013.

[21] I. Buist, J. McCourt, S. Potter, S. Ross and K. Trudel, "In situ burning," *Pure Applied Chemistry,* vol. 71, pp. 43-65, 1999.

[22] R. Wahi, L. Chuah, T. Choong, Z. Ngaini and M. Nourouzi, "Oil removal from aqueous state by natural fibrous sorbent: An overview," *Separation and Purification Technology,* vol. 113, pp. 51-63, 2013.

[23] J. Acevedo Cortez, B. Kharisov, T. Serrano Quezada and T. Hernández García, "Micro- and nanoporous materials capable of absorbing solvents and oils reversibly: the state of the art," *Petroleum Science,* vol. 14, pp. 84-104, 2017.

[24] T. Arbatan, X. Fang and W. Shen, "Superhydrophobic and oleophilic calcium carbonate powder as a selective oil sorbent with potential use in oil spill clean-ups," *Chemical Engineering Journal,* vol. 166, pp. 787-791, 2011.

[25] H. Li, L. Liu and F. Yang, "Hydrophobic modification of polyurethane foam for oil spill cleanup," *Marine Pollution Bulletin,* vol. 64, pp. 1648-1653, 2012.

[26] S. Banerjee, M. Joshi and R. Jayaram, "Treatment of oil spill by sorption technique using fatty acid grafted sawdust," *Chemosphere,* vol. 64, pp. 1026-1031, 2006.

[27] H. Liu, B. Geng, Y. Chen and H. Wang, "Review on the Aerogel-Type Oil Sorbents Derived from Nanocellulose," *ACS Sustainable Chem. Eng.,* vol. 5, p. 49–66, 2017.

[28] S. Gupta and N.-H. Tai, "Carbon materials as oil sorbents: a review on the synthesis and performance," *J. Mater. Chem. A,* vol. 4, pp. 1550-1565, 2016.

[29] H. Maleki, "Recent advances in aerogels for environmental remediation applications: A review," *Chemical Engineering Journal,* vol. 300, pp. 98-118, 2016.

[30] B. Okesola and D. Smith, "Applying low-molecular weight supramolecular gelators in an environmental setting – self-assembled gels as smart materials for pollutant removal," *Chem. Soc. Rev.,* vol. 45, pp. 4226-4251, 2016.

[31] D. Cornwell and D. Smith, "Expanding the scope of gels – combining polymers with low-molecular-weight gelators to yield modified self-assembling smart materials with high-tech applications," *Mater. Horiz.,* vol. 2, pp. 279-293, 2015.

[32] X. Yan, F. Wang, B. Zheng and F. Huang, "Stimuli-responsive supramolecular polymeric materials," *Chemical Society Reviews,* vol. 41, pp. 6042-6065, 2012.

[33] J. Raeburn, A. Cardoso and D. Adams, "The importance of the self-assembly process to control mechanical properties of low molecular weight hydrogels," *Chemical Society Reviews,* vol. 42, pp. 5143-5156, 2013.

[34] P. Rosales, M. Suidan and A. Venosa, "A laboratory screening study on the use of solidifiers as a response tool to remove crude oil slicks on seawater," *Chemosphere*, vol. 80, pp. 389-395, 2010.

[35] S. Mukherjee, C. Shang, X. Chen, X. Chang, K. Liu, C. Yu and Y. Fang, "N-Acetylglucosamine-based efficient, phase-selective organogelators for oil spill remediation," *Chemical Communications*, vol. 50, pp. 13940-13943, 2014.

[36] C. Raju, B. Pramanik, R. Ravishankar, P. Rao and G. Sriganesh, "Xylitol based phase selective organogelators for potential oil spillage recovery," *RSC Adv.*, vol. 7, pp. 37175-37180, 2017.

[37] A. Vibhute, V. Muvvala and K. Sureshan, "A Sugar-Based Gelator for Marine Oil-Spill Recovery," *Angew.Chem. Int. Ed.*, vol. 55, p. 7782 –7785, 2016.

[38] R. Belore, K. Trudel, J. Mullin and A. Guarino, "Large-scale cold water dispersant effectiveness experiments with Alaskan crude oils and Corexit 9500 and 9527 dispersants," *Marine Pollution Bulletin*, vol. 58, pp. 118-128, 2009.

[39] R. Lessard and G. DeMarco, "The Significance of Oil Spill Dispersants," *Spill Science & Technology Bulletin*, vol. 6, pp. 59-68, 2000.

[40] P. Venkataraman, J. Tang, E. Frenkel, G. McPherson, J. He, S. Raghavan, V. Kolesnichenko, A. Bose and V. John, "Attachment of a Hydrophobically Modified Biopolymer at the Oil–Water Interface in the Treatment of Oil Spills," *ACS Appl. Mater. Interfaces*, vol. 5, p. 3572–3580, 2013.

[41] S. Bratskaya, V. Avramenko, S. Schwarz and I. Philippova, "Enhanced flocculation of oil-in-water emulsions by hydrophobically modified chitosan derivatives," *Colloids and Surfaces A: Physicochemical and Engineering Aspects*, vol. 275, pp. 168-176, 2006.

[42] O. Owoseni, E. Nyankson, Y. Zhang, S. Adams, J. He, G. McPherson, A. Bose, R. Gupta and V. John, "Release of surfactant cargo from interfacially-active halloysite clay nanotubes for oil spill remediation," *Langmuir*, vol. 30, no. 45, p. 13533–13541, 2014.

[43] O. Laitinen, J. Ojala, J. Sirviö and H. Liimatainen, "Sustainable stabilization of oil in water emulsions by cellulose nanocrystals synthesized from deep eutectic solvents," *Cellulose*, vol. 24, p. 1679–1689, 2017.

[44] J. Ojala, J. Sirviö and H. Liimatainen, "Nanoparticle emulsifiers based on bifunctionalized cellulose nanocrystals as marine diesel oil–water emulsion stabilizers," *Chemical Engineering Journal*, vol. 288, pp. 312-320, 2016.

[45] T. Hunter, R. Pugh, G. Franks and G. Jameson, "The role of particles in stabilising foams and emulsions," *Advances in Colloid and Interface Science*, vol. 137, pp. 57-81, 2008.

[46] I. Tavernier, W. Wijaya, P. Van der Meeren, K. Dewettinck and A. Patel, "Food-grade particles for emulsion stabilization," *Trends in Food Science & Technology*, vol. 50, pp. 159-174, 2016.

[47] Y. Chevalier and M.-A. Bolzinger, "Emulsions stabilized with solid nanoparticles: Pickering emulsions," *Colloids and Surfaces A: Physicochemical and Engineering Aspects*, vol. 490, pp. 23-34, 2013.

[48] L. Botto, E. Lewandowski, M. Cavallaro and K. Stebe, "Capillary interactions between anisotropic particles," *Soft Matter*, vol. 8, p. 9957–9971, 2012.

[49] S. Lam, K. Velikov and O. Velev, "Pickering stabilization of foams and emulsions with particles of biological origin," *Current Opinion in Colloid & Interface Science*, vol. 19, pp. 490-500, 2014.

[50] A. Kumar, B. Park, F. Tu and D. Lee, "Amphiphilic Janus particles at fluid interfaces," *Soft Matter,* vol. 9, p. 6604–6617, 2013.

[51] M. Oettel and S. Dietrich, "Colloidal Interactions at Fluid Interfaces," *Langmuir,* vol. 24, pp. 1425-1441, 2008.

[52] R. Style, L. Isa and E. Dufresne, "Adsorption of soft particles at fluid interfaces," *Soft Matter,* vol. 11, pp. 7412--7419, 2015.

[53] S. Pickering, "Emulsions," *J. Chem. Soc.,* vol. 91, pp. 2001-2021, 1907.

[54] R. Aveyard, B. Binks and J. Clint, "Emulsions stabilised solely by colloidal particles," *Advances in Colloid and Interface Science,* Vols. 100-102, pp. 503-546, 2003.

[55] E. Dickinson, "Biopolymer-based particles as stabilizing agents for emulsions and foams," *Food Hydrocolloids,* vol. 68, pp. 219-231, 2017.

[56] M. Elsabee, R. Morsi and A. Al-Sabagh, "Surface active properties of chitosan and its derivatives," *Colloids and Surfaces B: Biointerfaces,* vol. 74, pp. 1-16, 2009.

[57] P. Schulz, M. Rodriguez, L. Del Blanco, M. Pistonesi and E. Agulló, "Emulsification properties of chitosan," *Colloid Polym Sci,* vol. 276, pp. 1159-1165, 1998.

[58] I. Pepic, J. Filipovic-Grcic and I. Jalsenjak, "Interactions in a nonionic surfactant and chitosan mixtures," *Colloids and Surfaces A: Physicochemical and Engineering Aspects,* vol. 327, pp. 95-102, 2008.

[59] C. Li, P. Sun and C. Yang, "Emulsion stabilized by starch nanocrystals," *Starch-Stärke,* vol. 64, no. 6, pp. 497-502, 2012.

[60] Y. Tan, K. Xu, C. Niu, C. Liu, Y. Li, P. Wang and B. Binks, "Triglycerideewater emulsions stabilised by starch-based nanoparticles," *Food Hydrocolloids,* vol. 36, pp. 70-75, 2014.

[61] I. Kalashnikova, H. Bizot, B. Cathala and I. Capron, "New Pickering emulsions stabilized by bacterial cellulose nanocrystals," *Langmuir,* vol. 27, no. 12, pp. 7471-7479, 2011.

[62] Z. Liu, Y. Jiao, Y. Wang, C. Zhou and Z. Zhang, "Polysaccharides-based nanoparticles as drug delivery systems," *Advanced Drug Delivery Reviews,* vol. 60, pp. 1650-1662, 2008.

[63] S. Mizrahy and D. Peer, "Polysaccharides as building blocks for nanotherapeutics," *Chem. Soc. Rev.,* vol. 41, pp. 2623-2640, 2012.

[64] E. Dickinson, "Food emulsions and foams: Stabilization by particles," *Current Opinion in Colloid & Interface Science,* vol. 15, pp. 40-49, 2010.

[65] J. Xiao, Y. Li and Q. Huang, "Recent advances on food-grade particles stabilized Pickering emulsions: Fabrication, characterization and research trends," *Trends in Food Science & Technology,* vol. 55, pp. 48-60, 2016.

[66] I. Joye and D. McClements, "Biopolymer-based nanoparticles and microparticles: Fabrication, characterization, and application," *Current Opinion in Colloid & Interface Science,* vol. 19, pp. 417-427, 2014.

[67] Y. Fang, R. Zhang, B. Duan, M. Liu, A. Lu and L. Zhang, "Recyclable Universal Solvents for Chitin to Chitosan with Various Degrees of Acetylation and Construction of Robust Hydrogels," *ACS Sustainable Chem. Eng.,* vol. 5, p. 2725−2733, 2017.

[68] R. Moon, A. Martini, J. Nairn, J. Simonsen and J. Youngblood, "Cellulose nanomaterials review: structure, properties and nanocomposites," *Chem. Soc. Rev.,* vol. 40, pp. 3941-3994, 2011.

[69] A. Buléon, P. Colonna, V. Planchot and S. Ball, "Starch granules: structure and biosynthesis," *International Journal of Biological Macromolecules,* vol. 23, pp. 85-112, 1998.

[70] D. Le Corre, J. Bras and A. Dufresne, "Starch Nanoparticles: A Review," *Biomacromolecules,* vol. 11, no. 5, pp. 1139-1153, 2010.

[71] J. Yang, S. Han, H. Zheng, H. Dong and J. Liu, "Preparation and application of micro/nanoparticles based on natural polysaccharides," *Carbohydrate Polymers,* vol. 123, p. 53–66, 2015.

[72] M. George and T. Abraham, "Polyionic hydrocolloids for the intestinal delivery of protein drugs: Alginate and chitosan — a review," *Journal of Controlled Release,* vol. 114, pp. 1-14, 2006.

[73] C. Goh, P. Heng and L. Chan, "Alginates as a useful natural polymer for microencapsulation and therapeutic applications," *Carbohydrate Polymers,* vol. 88, pp. 1-12, 2012.

[74] I. Joye and D. McClements, "Production of nanoparticles by anti-solvent precipitation for use in food systems," *Trends in Food Science & Technology,* vol. 34, pp. 109-123, 2013.

[75] A. Thorat and S. Dalvi, "Liquid antisolvent precipitation and stabilization of nanoparticles of poorly water soluble drugs in aqueous suspensions: Recent developments and future perspective," *Chemical Engineering Journal,* Vols. 181-182, pp. 1-34, 2012.

[76] M. Tzoumaki, T. Moschakis, V. Kiosseoglou and C. Biliaderis, "Oil-in-water emulsions stabilized by chitin nanocrystal particles," *Food Hydrocolloids,* vol. 25, no. 6, pp. 1521-1529, 2011.

[77] M. Tzoumaki, T. Moschakis, E. Scholten and C. Biliaderis, "In vitro lipid digestion of chitin nanocrystal stabilized o/w emulsions," *Food & Function,* vol. 4, no. 1, pp. 121-129, 2013.

[78] A. Salaberria, J. Labidi and S. Fernandes, "Different routes to turn chitin into stunning nano-objects," *European Polymer Journal,* vol. 68, p. 503–515, 2015.

[79] H. Liu, C. Wang, S. Zou, Z. Wei and Z. Tong, "Simple, Reversible Emulsion System Switched by pH on the Basis of Chitosan without Any Hydrophobic Modification," *Langmuir,* vol. 28, p. 11017−11024, 2012.

[80] W. Mwangi, K.-W. Ho, B.-T. Tey and E.-S. Chan, "Effects of environmental factors on the physical stability of pickering-emulsions stabilized by chitosan particles," *Food Hydrocolloids,* vol. 60, pp. 543-550, 2016.

[81] K. Ho, C.-W. Ooi, W. Mwangi, W. Leong, B.-T. Tey and E.-S. Chan, "Comparison of self-aggregated chitosan particles prepared with and without ultrasonication pretreatment as Pickering emulsifier," *Food Hydrocolloids,* vol. 52, pp. 827-837, 2016.

[82] X.-Y. Wang and M.-C. Heuzey, "Chitosan-Based Conventional and Pickering Emulsions with Long-Term Stability," *Langmuir,* vol. 32, p. 929−936, 2016.

[83] A. Kumari, S. Yadav and S. Yadav, "Biodegradable polymeric nanoparticles based drug delivery systems," *Colloids and Surfaces B: Biointerfaces,* vol. 75, pp. 1-18, 2010.

[84] M. Amidi, E. Mastrobattista, W. Jiskoot and W. Hennink, "Chitosan-based delivery systems for protein therapeutics and antigens," *Advanced Drug Delivery Reviews,* vol. 62, pp. 59-82, 2010.

[85] W. Fan, W. Yan, Z. Xu and H. Ni, "Formation mechanism of monodisperse, low molecular weight chitosan nanoparticles by ionic gelation technique," *Colloids and Surfaces B: Biointerfaces,* vol. 90, p. 21– 27, 2012.

[86] Q. Gan, T. Wang, C. Cochrane and P. McCarron, "Modulation of surface charge, particle size and morphological properties of chitosan–TPP nanoparticles intended for gene delivery," *Colloids and Surfaces B: Biointerfaces,* vol. 44, pp. 65-73, 2005.

[87] Y. Huang, Y. Cai and Y. Lapitsky, "Factors affecting the stability of chitosan/tripolyphosphate micro- and nanogels: resolving the opposing findings," *Journal of Materials Chemistry B,* vol. 3, pp. 5957-5970, 2015.

[88] Z. He, J. Santos, H. Tian, H. Huang, Y. Hu, L. Liu, K. Leong, Y. Chen and H.-Q. Mao, "Scalable fabrication of size-controlled chitosan nanoparticles for oral delivery of insulin," *Biomaterials,* vol. 130, pp. 28-41, 2017.

[89] C. Sipoli, N. Santana, A. Shimojo, A. Azzoni and L. de la Torre, "Scalable production of highly concentrated chitosan/TPP nanoparticles in different pHs and evaluation of the in vitro transfection efficiency," *Biochemical Engineering Journal,* vol. 94, pp. 65-73, 2015.

[90] Y. Dong, W. Ng, S. Shen, S. Kim and R. Tan, "Scalable ionic gelation synthesis of chitosan nanoparticles for drug delivery in static mixers," *Carbohydrate Polymers,* vol. 94, pp. 940-945, 2013.

[91] B. Riegger, B. Bäurer, A. Mirzayeva, G. Tovar and M. Bach, "A systematic approach of chitosan nanoparticle preparation via emulsion crosslinking as potential adsorbent in wastewater treatment," *Carbohydrate Polymers,* vol. 180, pp. 46-54, 2018.

[92] B. Shah, Y. Li, W. Jin, Y. An, L. He, Z. Li, W. Xu and B. Li, "Preparation and optimization of Pickering emulsion stabilized by chitosan-tripolyphosphate nanoparticles for curcumin encapsulation," *Food Hydrocolloids,* vol. 52, pp. 369-377, 2016.

[93] X. Chen and H. Park, "Chemical characteristics of O-carboxymethyl chitosans related to the preparation conditions," *Carbohydr. Polym.*, vol. 53, pp. 355-259, 2003.

[94] L. Upadhyaya, J. Singh, V. Agarwal and R. Tewari, "The implications of recent advances in carboxymethyl chitosan based targeted drug delivery and tissue engineering applications," *Journal of Controlled Release,* vol. 186, pp. 54-87, 2014.

[95] V. Mourya, N. Inamdar and A. Tiwari, "Carboxymethyl chitosan and its applications," *Adv. Mat. Lett.*, vol. 1, pp. 11-33, 2010.

[96] V. Mourya and N. Inamdar, "Chitosan-modifications and applications: Opportunities galore," *Reactive & Functional Polymers,* vol. 68, p. 1013–1051, 2008.

[97] C. Yu, L. Yun-fei, T. Hui-min and J. Jian-xin, "Synthesis and characterization of a novel superabsorbent polymer of N,O-carboxymethyl chitosan graft copolymerized with vinyl monomers," *Carbohydrate Polymers,* vol. 75, p. 287–292, 2009.

[98] X. Shi, Y. Du, J. Yang, B. Zhang and L. Sun, "Effect of degree of substitution and molecular weight of carboxymethyl chitosan nanoparticles on doxorubicin delivery," *Journal of Applied Polymer Science,* vol. 100, p. 4689–4696, 2006.

[99] J. Wang, J. Chen, J. Zong, D. Zhao, F. Li, R. Zhuo and S. Cheng, "Calcium Carbonate/Carboxymethyl Chitosan Hybrid Microspheres and Nanospheres for Drug Delivery," *Journal of Physical Chemistry C,* vol. 114, p. 18940–18945, 2010.

[100] A. Anitha, V. V. Divya Rani, R. Krishna, V. Sreeja, N. Selvamurugan, S. V. Nair, H. Tamura and R. Jayakumar, "Synthesis, characterization, cytotoxicity and antibacterial

studies of chitosan, O-carboxymethyl and N,O-carboxymethyl chitosan nanoparticles," *Carbohydrate Polymers,* vol. 78, p. 672–677, 2009.

[101] A. Anitha, S. Maya, K. Chennazhi, S. Nair, H. Tamura and R. Jayakumar, "Efficient water soluble O-carboxymethyl chitosan nanocarrier for the delivery of curcumin to cancer cells," *Carbohydrate Polymers,* vol. 83, pp. 452-461, 2011.

[102] Z. Teng, Y. Luo and Q. Wang, "Carboxymethyl chitosan–soy protein complex nanoparticles for the encapsulation and controlled release of vitamin D3," *Food Chemistry,* vol. 141, p. 524–532, 2013.

[103] Y.-C. Huang and T.-H. Kuo, "O-carboxymethyl chitosan/fucoidan nanoparticles increase cellular curcumin uptake," *Food Hydrocolloids,* vol. 53, pp. 261-269, 2016.

[104] A. Jimtaisong and N. Saewan, "Utilization of carboxymethyl chitosan in cosmetics," *International Journal of Cosmetic Science,* vol. 36, pp. 12-21, 2014.

[105] A. Dufresen and J. Castano, "Polysaccharide nanomaterial reinforced starch nanocomposites: A review," *Starch/Stärke,* vol. 69, pp. 1-19, 2017.

[106] H. Sashiwa, N. Yamamori, Y. Ichinose, J. Sunamoto and S. Aiba, "Michael Reaction of Chitosan with Various Acryl Reagents in Water," *Biomacromolecules,* vol. 4, pp. 1250-1254, 2003.

Publication I

Kalliola S., Repo E., Sillanpää M., Arora J.S., He J., John V.T.
The stability of green nanoparticles in increased pH and salinity for applications in oil spill-treatment

Reprinted with permission from
Colloids and Surfaces A: Physicochemical and Engineering Aspects 493
Vol. 493, pp. 99-107, 2015

Publication II

Kalliola S., Repo E., Srivastava V., Heiskanen J.P., Sirviö J.A., Liimatainen H., Sillanpää M.
The pH sensitive properties of carboxymethyl chitosan nanoparticles cross-linked with calcium ions

Reprinted with permission from
Colloids and Surfaces B: Biointerfaces
Vol. 153, pp. 229-236, 2016

Publication III

Kalliola S., Repo E., Srivastava V., Zhao F., Heiskanen J.P., Sirviö J.A., Liimatainen H., Sillanpää M.

Carboxymethyl chitosan and its hydrophobically modified derivative as pH-switchable emulsifiers

Reprinted with permission from
Langmuir
Vol. 34(8), pp. 2800–2806, 2018

Publication IV

Kalliola S., Repo E., Zhao F., Srivastava V., Sillanpää M.
Vanillin substituted chitosan particles applied to oil/water separation

Submitted to
Reactive and Functional Polymers

ACTA UNIVERSITATIS LAPPEENRANTAENSIS

793. AJO, PETRI. Hydroxyl radical behavior in water treatment with gas-phase pulsed corona discharge. 2018. Diss.

794. BANAEIANJAHROMI, NEGIN. On the role of enterprise architecture in enterprise integration. 2018. Diss.

795. HASHEELA-MUFETI, VICTORIA TULIVAYE. Empirical studies on the adoption and implementation of ERP in SMEs in developing countries. 2018. Diss.

796. JANHUNEN, SARI. Determinants of the local acceptability of wind power in Finland. 2018. Diss.

797. TEPLOV, ROMAN. A holistic approach to measuring open innovation: contribution to theory development. 2018. Diss.

798. ALBATS, EKATERINA. Facilitating university-industry collaboration with a multi-level stakeholder perspective. 2018. Diss.

799. TURA, NINA. Value creation for sustainability-oriented innovations: challenges and supporting methods. 2018. Diss.

800. TALIKKA, MARJA. Recognizing required changes to higher education engineering programs' information literacy education as a consequence of research problems becoming more complex. 2018. Diss.

801. MATTSSON, ALEKSI. Design of customer-end converter systems for low voltage DC distribution from a life cycle cost perspective. 2018. Diss.

802. JÄRVI, HENNA. Customer engagement, a friend or a foe? Investigating the relationship between customer engagement and value co-destruction. 2018. Diss.

803. DABROWSKA, JUSTYNA. Organizing for open innovation: adding the human element. 2018. Diss.

804. TIAINEN, JONNA. Losses in low-Reynolds-number centrifugal compressors. 2018. Diss.

805. GYASI, EMMANUEL AFRANE. On adaptive intelligent welding: Technique feasibility in weld quality assurance for advanced steels. 2018. Diss.

806. PROSKURINA, SVETLANA. International trade in biomass for energy production: The local and global context. 2018. Diss.

807. DABIRI, MOHAMMAD. The low-cycle fatigue of S960 MC direct-quenched high-strength steel. 2018. Diss.

808. KOSKELA, VIRPI. Tapping experiences of presence to connect people and organizational creativity. 2018. Diss.

809. HERALA, ANTTI. Benefits from Open Data: barriers to supply and demand of Open Data in private organizations. 2018. Diss.

810. KÄYHKÖ, JORMA. Erityisen tuen toimintaprosessien nykytila ja kehittäminen suomalaisessa oppisopimuskoulutuksessa. 2018. Diss.

811. HAJIKHANI, ARASH. Understanding and leveraging the social network services in innovation ecosystems. 2018. Diss.

812. SKRIKO, TUOMAS. Dependence of manufacturing parameters on the performance quality of welded joints made of direct quenched ultra-high-strength steel. 2018. Diss.

813. KARTTUNEN, ELINA. Management of technological resource dependencies in interorganizational networks. 2018. Diss.

814. CHILD, MICHAEL. Transition towards long-term sustainability of the Finnish energy system. 2018. Diss.

815. NUTAKOR, CHARLES. An experimental and theoretical investigation of power losses in planetary gearboxes. 2018. Diss.

816. KONSTI-LAAKSO, SUVI. Co-creation, brokering and innovation networks: A model for innovating with users. 2018. Diss.

817. HURSKAINEN, VESA-VILLE. Dynamic analysis of flexible multibody systems using finite elements based on the absolute nodal coordinate formulation. 2018. Diss.

818. VASILYEV, FEDOR. Model-based design and optimisation of hydrometallurgical liquid-liquid extraction processes. 2018. Diss.

819. DEMESA, ABAYNEH. Towards sustainable production of value-added chemicals and materials from lignocellulosic biomass: carboxylic acids and cellulose nanocrystals. 2018. Diss.

820. SIKANEN, EERIK. Dynamic analysis of rotating systems including contact and thermal-induced effects. 2018. Diss.

821. LIND, LOTTA. Identifying working capital models in value chains: Towards a generic framework. 2018. Diss.

822. IMMONEN, KIRSI. Ligno-cellulose fibre poly(lactic acid) interfaces in biocomposites. 2018. Diss.

823. YLÄ-KUJALA, ANTTI. Inter-organizational mediums: current state and underlying potential. 2018. Diss.

824. ZAFARI, SAHAR. Segmentation of partially overlapping convex objects in silhouette images. 2018. Diss.

825. MÄLKKI, HELENA. Identifying needs and ways to integrate sustainability into energy degree programmes. 2018. Diss.

826. JUNTUNEN, RAIMO. LCL filter designs for paraller-connected grid inverters. 2018. Diss.

827. RANAEI, SAMIRA. Quantitative approaches for detecting emerging technologies. 2018. Diss.

828. METSO, LASSE. Information-based industrial maintenance - an ecosystem perspective. 2018. Diss.

829. SAREN, ANDREY. Twin boundary dynamics in magnetic shape memory alloy Ni-Mn-Ga five-layered modulated martensite. 2018. Diss.

830. BELONOGOVA, NADEZDA. Active residential customer in a flexible energy system - a methodology to determine the customer behaviour in a multi-objective environment. 2018. Diss.

Acta Universitatis
Lappeenrantaensis
831

LUT University

ISBN 978-952-335-308-4
ISBN 978-952-335-309-1 (PDF)
ISSN-L 1456-4491
ISSN 1456-4491
Lappeenranta 2018